


For Reference

NOT TO BE TAKEN FROM THIS ROOM



Digitized by the Internet Archive
in 2023 with funding from
University of Alberta Library

https://archive.org/details/Islam1982_0

THE UNIVERSITY OF ALBERTA

RELEASE FORM

NAME OF AUTHOR F. A. ISLAM

TITLE OF THESIS Errors obtained by using the standard theory to calculate absorption coefficients in the dynamical theory of electron diffraction which includes non-systematic reflections.

DEGREE FOR WHICH THESIS WAS PRESENTED M.Sc.

YEAR THIS DEGREE GRANTED Fall, 1982

Permission is hereby granted to THE UNIVERSITY OF ALBERTA LIBRARY to reproduce single copies of this thesis and to lend or sell such copies for private, scholarly or scientific research purposes only.

The author reserves other publication rights, and neither the thesis nor extensive extracts from it may be printed or otherwise reproduced without the author's written permission.

THE UNIVERSITY OF ALBERTA

Errors obtained by using the standard theory to calculate
absorption coefficients in the dynamical theory of electron
diffraction which includes non-systematic reflections.

by



F. A. ISLAM

A THESIS

SUBMITTED TO THE FACULTY OF GRADUATE STUDIES AND RESEARCH
IN PARTIAL FULFILMENT OF THE REQUIREMENTS FOR THE DEGREE
OF Master of Science.

Department of Physics

EDMONTON, ALBERTA

Fall, 1982

THE UNIVERSITY OF ALBERTA
FACULTY OF GRADUATE STUDIES AND RESEARCH

The undersigned certify that they have read, and recommend to the Faculty of Graduate Studies and Research, for acceptance, a thesis entitled Errors obtained by using the standard theory to calculate absorption coefficients in the dynamical theory of electron diffraction which includes non-systematic reflections. submitted by F. A. ISLAM in partial fulfilment of the requirements for the degree of Master of Science..

ABSTRACT

A comparison of the standard and exact methods for taking absorption into account has been carried out for the cases where Bloch wave degeneracies occur due to the presence of non-systematic reflections. Diffraction conditions have been chosen so that only three beams need be taken into account in the calculations. All the calculations have been carried out for materials of differing atomic number. When the reflection chosen for dark field image (referred as the systematic reflection in this thesis) is in its Bragg condition two degenerate Bloch waves are obtained. Under these circumstances it has been found that the results obtained from the standard and exact methods are in good agreement with one another.

When the systematic reflection is close to its Bragg condition, the two Bloch waves are nearly degenerate. Under these circumstances marked differences have been found between the results obtained from the two methods. These differences have been found to increase with increasing atomic number.

In a study of the effect of higher order non-systematic reflections it has been found that the differences in the results obtained from the two methods increase with increasing order of non-systematic reflections.

ACKNOWLEDGEMENT

I wish to express my sincere gratitude to Dr. S.S.Shienin, my research supervisor for his continual help, interest and encouragement during the course of this work.

In addition I would like to thank Mr.R. Perez for his helpful discussion and sugestions.

Finally, I wish to thank the National Research Council of Canada and the University of Alberta for financial support throughout the course of this project.

TABLE OF CONTENTS

CHAPTER 1	1
1.1 INTRODUCTION	1
1.2 Scope of the present investigation	6
CHAPTER 2	
ASPECTS OF THE DYNAMICAL THEORY OF ELECTRON DIFFRACTION	7
2.1 Basic outline of the Dynamical Theory	7
2.2 The Calculation of Diffracted Beam Intensities in a Perfect Crystal	14
2.2.1 Systematic and Non-systematic Reflections ..	17
2.3 Relativistic Corrections To The Dynamical Theory ..	20
CHAPTER 3	
EFFECTS OF INELASTIC SCATTERING	22
3.1 Introduction	22
3.2 The Standard Theory for Taking Absorption into Account	22
3.2.1 Anomalous Absorption	26
3.3 Exact method for Taking Absorption into Account ..	29
3.3.1 Calculation of Diffracted Beam Intensities ..	31
CHAPTER 4	
THEORETICAL CALCULATIONS	33
4.1 Introduction	33

4.2	Setting up the A matrix	33
4.2.1	Calculation of the Diagonal Elements of A Matrix	33
4.2.2	The Calculation Of The Off-Diagonal Elements Of The A Matrix	39
4.3	Setting up the B matrix	40
4.4	Diagonalization of matrices A and B	40
4.5	Reflections chosen in the calculations	41
4.6	Diffraction conditions for which the Bloch wave degeneracies are obtained	44
4.7	Calculation of Absorption coefficients, Excitation amplitude and Diffracted beam intensity using the Standard method	48
4.8	Calculation of Absorption coefficients, Excitation amplitude and Diffracted beam Intensity using the exact method	49

CHAPTER 5

RESULTS AND DISCUSSION	50
5.1 Introduction	50
5.2 A Comparison of Absorption coefficients, Excitation amplitudes and Diffracted beam intensities obtained with Standard and Exact methods.	51
5.2.1 The case of degenerate diffraction conditions	51
5.2.2 Results in the case of quasi-degenerate	

diffraction conditions	57
5.2.3 Results in the multi-beam case	68
5.2.4 Effects of higher order non-systematic reflection	68
5.3 Discussion	75
5.3.1 A discussion of the effect of order of the non-systematic reflections on absorption coefficients when the systematic reflection is close to its Bragg condition.	76
5.4 Conclusions	79
References	82

List of Tables

Table

page

1. Percentage differences in the absorption coefficients and diffracted beam intensities calculated by using both standard and exact methods at the point where Bloch waves 2 and 3 are degenerate. Three beam calculations were used and the results shown are for silicon, copper and gold. 56
2. Percentage differences in absorption coefficients and diffracted beam intensities calculated by using standard and exact method at a point where Bloch waves 2 and 3 are quasi-degenerate. 3 beam and 11 beam calculations were used and the results shown are for Si, Cu and Au. 65
3. Percentage differences in absorption coefficient and diffracted beam intensities calculated by using standard and exact method for the cases where Bloch waves 2 and 3 are both degenerate and quasi-degenerate. 3 beam calculations were used including (000), (220) and ($\bar{1}$ 37) reflections and the results shown are for Si and Cu. 71
4. Percentage differences in diffracted beam intensities calculated by using standard and exact method at the point where Bloch waves 2 and 3 are quasi-degenerate. 3 beam calculations were used and the results shown are for Cu. 73

5. Percentage differences in diffracted beam intensities calculated by using standard and exact method at the point where Bloch waves 2 and 3 are quasi-degenerate. 3 beam calculations were used and the results shown are for Cu. 74
6. B matrices for three beam calculation in which (a) (000), (220), ($\bar{1}33$) and (b) (000), (220), ($\bar{1}37$) reflections are included. 77

List of Figures

Figure		page
1.	The dispersion surface and the Ewald sphere construction for high energy electrons. $w^{(1)}_{\text{T}} = \gamma^{(1)}$ and $w^{(2)}_{\text{T}} = \gamma^{(2)}$	12
2.	A computed diffraction pattern for [310] orientation in a crystal with fcc structure.	19
3.	A schematic diagram showing the paths of electrons scattered inelastically outside the objective aperture (as for example AA').	24
4.	The variation of diffracted beam intensity with thickness when (a) no absorption (b) normal absorption and (c) anomalous absorption is taken into account.	28
5.	The intersection of the Ewald sphere with the zero order Laue zone. The orientation is specified by the tie point method. The point L is the perpendicular projection of the centre of the Ewald sphere(tie-point) on the zero order Laue plane.	35
6.	The dispersion surface and the Ewald sphere construction showing parameters required for calculation of diagonal elements of the \underline{A} matrix.	37
7.	A computed diffraction pattern for a [334] orientation in a crystal with fcc structure showing the 11 reflections which were considered in the many beam calculations.	43

8. The variation of $\gamma^{(i)}$ ($i = 1, 2, 3$) with $\Delta\theta_{\bar{1}33}$ as given by a three beam calculation including (000), (220), and ($\bar{1}33$) reflections. $\Delta\theta_{220} = 0.0$. 47
9. The variation of $\gamma^{(i)}$ ($i = 1, 2, 3$) with $\Delta\theta_{\bar{1}33}$ as given by a three beam calculation including the (000), (220), and ($\bar{1}33$) reflections. $\Delta\theta_{220} = -0.1\theta_{220}$. 47
10. The variation of excitation amplitude $|\phi_{220}^{(i)}|$ ($i = 2, 3$) with $\Delta\theta_{\bar{1}33}$ for Cu, at $\Delta\theta_{220} = 0$ calculated by (a) the standard and (b) the exact methods. 53
11. The variation of Bloch wave absorption coefficients $q^{(i)}$ with $\Delta\theta_{\bar{1}33}$ for Cu, at $\Delta\theta_{220} = 0$, calculated by using (a) the standard and (b) the exact methods. 55
12. The variation of (a) excitation amplitude $|\phi_{220}^{(i)}|$ ($i = 2, 3$) and (b) the variation of $q^{(i)}$ ($i = 2, 3$) with $\Delta\theta_{\bar{1}33}$. Calculations were carried out for Cu using both exact and standard methods, at a value of $\Delta\theta_{220} = -0.0001\theta_{220}$ 59
13. The variation of diffracted beam intensity with crystal thickness for Cu obtained by using the standard and exact methods. Calculations were carried out at the point where Bloch waves 2 and 3 are quasi-degenerate i.e., at $\Delta\theta_{\bar{1}33} = -0.05\theta_{\bar{1}33}$ and $\Delta\theta_{220} = -0.0001\theta_{220}$. 61
14. The variation of diffracted beam intensity with crystal thickness for Si obtained by using the standard and exact methods. Calculations were

carried out at the point where Bloch waves 2 and 3 are quasi-degenerate i.e., at $\Delta\theta_{\bar{1}33} = -0.05 \theta_{\bar{1}33}$ and $\Delta\theta_{220} = -0.0001 \theta_{220}$. 64

15. The variation of diffracted beam intensity with crystal thickness for Au obtained by using the standard and exact methods. Calculations were carried out at the point where Bloch waves 2 and 3 are quasi-degenerate i.e., at $\Delta\theta_{\bar{1}33} = -0.115 \theta_{\bar{1}33}$ and $\Delta\theta_{220} = -0.0001 \theta_{220}$. 64

16(a).

The variation of the Bloch wave absorption coefficients $q^{(i)}$ with $\Delta\theta_{\bar{1}33}$ for Cu at $\Delta\theta_{220} = -0.0001\theta_{220}$, calculated by using both standard and exact methods. 11 beams were taken into account in the calculations. 67

16(b).

The variation of diffracted beam intensity with crystal thickness for Cu obtained by using the standard and exact methods. Calculations were carried out at the point where Bloch waves 2 and 3 are quasi-degenerate i.e., at $\Delta\theta_{\bar{1}33} = -0.03 \theta_{\bar{1}33}$ and $\Delta\theta_{220} = -0.0001 \theta_{220}$. 11 beam were taken into account in the calculations. 67

17(a).

The variation of the Bloch wave absorption coefficients $q^{(i)}$ with $\Delta\theta_{\bar{1}37}$ for Cu. Calculations were carried out by using both standard and exact

methods at a value of $\Delta\theta_{220} = -0.0001\theta_{220}$

70

17(b).

The variation of diffracted beam intensity with crystal thickness for Cu obtained by using the standard and exact methods. Calculations were carried out at the point where Bloch waves 2 and 3 are quasi-degenerate i.e., at $\Delta\theta_{137} = -0.03\theta_{137}$ and $\Delta\theta_{220} = -0.0001\theta_{220}$.

70

CHAPTER 1

1.1 INTRODUCTION

The electron microscope is an important tool in the study of the structure of materials. In order for the microscopist to interpret the experimental micrographs obtained from his instrument, it is necessary that reference be made to some theory which relates image contrast to specimen structure. The interpretation of electron micrographs of crystalline materials in terms of electron diffraction theories has played an important role in the development of electron microscopy as applied to problems in material science. Initially, after the development of the electron microscope by Knoll and Ruska(1932), the interpretation of the images obtained from crystalline specimens was carried out in terms of the kinematical theory of electron diffraction. This theory is similar to the kinematical theory of X-ray diffraction which had been used successfully to explain many aspects of the interaction of X-rays and crystals. However a number of authors(for example, Blackman 1939; Von Borries and Ruska. 1940; Heidenreich, 1942; Hillier and Baker, 1942; Boersch 1942,1943; Kinder,1943; Heidenreich and Sturkey, 1945) reported experimental results which could only be partially

explained in terms of the kinematical theory. As a result, an interest was developed in the dynamical theory of electron diffraction (Bethe 1928). Although this theory will be described in detail in chapter 2, for the present it is useful to note that Bethe's approach is quantum mechanical in nature and is based on the interaction of fast electrons with a crystal as described by the Schrodinger wave equation. The wave functions are Bloch waves of the form

$$\psi^{(i)} = \sum_{\vec{g}} C_{\vec{g}}^{(i)} \exp(2\pi i (\vec{k}^{(i)} + \vec{g}) \cdot \vec{r}) \quad (1.1)$$

where \vec{g} is a reciprocal lattice vector, $\vec{k}^{(i)}$ is a Bloch wave vector and $C_{\vec{g}}^{(i)}$ is a Bloch wave Fourier coefficient in the direction $\vec{k}^{(i)} + \vec{g}$. In solving the Shrodinger equation, the lattice potential is expressed as Fourier series which can be written as

$$V(\vec{r}) = \sum_{\vec{g}} V_{\vec{g}} \exp(2\pi i \vec{g} \cdot \vec{r}) \quad (1.2)$$

where $V_{\vec{g}}$ is a Fourier coefficient of the lattice potential.

Bethe's formulation of the dynamical theory does not take the effects of inelastic scattering into account. Some of the inelastically scattered electrons will be scattered outside the objective aperture and therefore do not contribute to the image (see fig.3, chapter 3). These

electrons are therefore effectively absorbed and it is in this context that the term absorption is used in this thesis. As will be shown in chapter 3, absorption can be taken into account in the dynamical theory by the introduction of an imaginary part of the lattice potential (Kambe and Molière, 1970; Dederichs, 1972). The lattice potential is then complex and can be written as

$$V(\vec{r}) + iV'(\vec{r}) = \sum_{\vec{g}} (V_{\vec{g}} + iV'_{\vec{g}}) \exp(2\pi i \vec{g} \cdot \vec{r}) \quad (1.3)$$

Another important aspect of the theory is the manner in which the imaginary Fourier coefficient $iV'_{\vec{g}}$ of equation (1.3) is incorporated in the theory. The approach widely used in the literature is to assume that the imaginary part of the lattice potential is much smaller than the real part, thus permitting first order perturbation theory for non degenerate states to be used (Hirsch et. al, 1965). This method is referred as the standard method in the literature. However this form of perturbation theory is only applicable to the diffraction conditions for which Bloch wave degeneracies do not occur (in this thesis the Bloch wave degeneracy will be taken to mean an equality in the kinetic energies of the Bloch waves (see equation 2.15, chapter 2)). In most work performed in the past Bloch wave degeneracies were not taken into consideration. As a result the standard

method for calculating absorption coefficients, based on first order perturbation theory for non-degenerate states, has been found to be adequate. During the last several years, however there has been considerable interest in phenomena, such as the critical voltage effect (Lally et.al 1972, Andrew and Sheinin 1974A) in which the occurrence of a Bloch wave degeneracy is involved. Bloch wave degeneracies are also found to occur when non-systematic reflections are taken into account in the dynamical theory (Gjonnes and Hoier 1971; Cann and Sheinin 1972; Sprague and Wilkins 1970) (for definition of non-systematic reflection see section 2.2.1, chapter 2). Sheinin and Cann (1973) and Serneels and Gevers (1973) have suggested that perturbation theory for doubly degenerate states could be used in evaluating absorption coefficients in critical voltage calculations. This theory overcomes the difficulty of infinite correction to the eigenvectors referred to by Sprague and Wilkins (1970). An alternative approach is to solve the Schrodinger equation including complex potential without making any approximation about the size of the perturbation or about how close the kinetic energies of the Bloch waves are to one another. This method is referred as exact method in this thesis. In this method there are two approaches to the solution of the Schrodinger equation. These are

- a. diagonalizing the complex matrix directly (Lally et.al 1972; Thomas 1972) and
- b. using generalized perturbation theory(Andrew and Sheinin 1975).

The second approach is more useful than the first since it gives some insight into the interaction between the Bloch waves which results from the introduction of the complex lattice potential.

In a comparison of critical voltage calculations based on the standard method with those obtained from the method based on exact theory, Lally et.al.(1972) and Andrew and Sheinin(1974A) found that errors obtained by using the standard method are small in the lighter elements but in a heavy element such as gold, significant errors were obtained. Sheinin and Cann(1973) found that significant errors could also be obtained in diffracted beam intensity calculations in which non-systematic reflections were taken into account. A detail investigation of the nature of these errors has, however, not been presented in the literature. Because the standard theory is so widely used in diffracted beam intensity calculations, it was felt important that such a study be carried out. The present work was undertaken with this in mind.

1.2 Scope of the present investigation

In order to carry out an investigation of the errors obtained in using the standard theory for the case when non-systematic reflections are taken into account, a comparison of calculations based on standard method with those based on exact method has been carried out:

- a. for diffraction conditions for which a Bloch wave degeneracy occurs in the presence of a non-systematic reflection,
- b. for diffraction condition for which two Bloch waves are quasi-degenerate (nearly degenerate or having close eigenvalues),
- c. for elements of different crystal structure and of differing atomic number and
- d. for both low order and higher order non-systematic reflections.

CHAPTER 2

ASPECTS OF THE DYNAMICAL THEORY OF ELECTRON DIFFRACTION

2.1 Basic outline of the Dynamical Theory

The dynamical theory of electron diffraction, as first proposed by Bethe(1928) and further developed by Macgillavry (1940) and Heidenreich(1949) starts with the Schrodinger equation for an electron in a crystal potential $V(\vec{r})$. Since the crystal potential $V(\vec{r})$ is periodic in nature, it can be expressed in the form of a Fourier series as follows

$$\begin{aligned} V(\vec{r}) &= \sum_{\vec{g}} V_{\vec{g}} \exp(2\pi i \vec{g} \cdot \vec{r}) \\ &= (h^2/(2me)) \sum_{\vec{g}} U_{\vec{g}} \exp(2\pi i \vec{g} \cdot \vec{r}) \end{aligned} \quad (2.1)$$

where the summation is over all reciprocal lattice vector \vec{g} . If only elastic scattering is considered, the crystal potential is real, $V(\vec{r}) = V^*(\vec{r})$, and therefore,

$$U_{\vec{g}} = U_{-\vec{g}}^* \quad (2.2)$$

In addition if the crystal has a centre of symmetry at the origin, $V(\vec{r}) = V(-\vec{r})$ and

$$U_g = U_{-g} = U_g^* \quad (2.3)$$

Outside the crystal, where $V(\vec{r}) = 0$, the solution of the Schrodinger equation is a plane wave of the form

$$\psi(\vec{r}) = \exp(2\pi i \vec{\chi} \cdot \vec{r}) \quad (2.4)$$

where magnitude of the wave vector $\vec{\chi}$ is such that

$$(\hbar^2 \chi^2)/2m = eE \quad (2.5)$$

where E is the potential through which the electron was accelerated before entering the crystal. In the crystal the electron wave functions are Bloch waves, that is plane waves modulated by a function which has the periodicity of the lattice. Accordingly the solutions to the Schrodinger equation are of the form of equation(1.1)(see chapter 1). If the expression for $V(\vec{r})$ and $\psi(\vec{r})$ are substituted in the Schrodinger equation, a set of equations is obtained which can be written as

$$(\hbar^2 K^2 - (\hbar^2 \vec{k}_g^{(i)})^2) C_g^{(i)} + \sum'_h U_h C_{g-h}^{(i)} = 0 \quad (2.6)$$

where prime on the summation indicates that the term $h = 0$ is excluded and

where

$$K^2 = \chi^2 + U_0 \quad (2.7)$$

$$\vec{k}_g^{(i)} = \vec{k}^{(i)} + \vec{g} \quad (2.8)$$

K is the magnitude of the electron wavevector in the crystal after correcting for mean crystal potential. This homogenous set of equations gives the general relationship between the Bloch wave Fourier coefficients $C_g^{(i)}$, the Fourier coefficients of lattice potential U_g and the Bloch wave vectors $\vec{k}^{(i)}$. These equations (2.6) are referred as the 'dispersion equations' by Bethe (1928).

Now the question which arises at this point is what approach should be taken in solving the set of equations (2.6). One approach which have been extensively used in the past (Whelan and Hirsch 1957; N. Kato 1952) is to assume that only two beams are important. Under these circumstances the set of equations (2.6) consists of only two equations for which analytical solutions exist. However in the present work we are primarily interested in studying the effects of non-systematic reflections (see section 2.2.1) and therefore more than two beams must be taken into account. If N diffracted beams are considered then (2.6) consists of N equations for which analytical solutions generally can not be found. Numerical solutions of these equations must

therefore be adopted. There have been a number of formulations of the multi-beam dynamical theory which can be used to obtain such numerical solutions (see for example Sturkey(1957), Fujimoto (1959)). The formulation employed in the present work is based on expressing (2.6) in the form of an eigenvalue equation(Howie and Whelan 1961). This formulation is particularly useful since any number of beams can be included and the form of the equation leads itself to straightforward numerical solution.

The manner in which the eigenvalue equation is derived can be understood by considering Fig.1 . The values of $\vec{k}^{(i)}$ satisfying (2.6) lie on a surface called the dispersion surface. The wave points of the Bloch wave excited inside the crystal are obtained from the condition that the tangential components of the Bloch wave vectors must be equal to that of the incident beam. Thus a line is drawn through the point T (in fig.1) and perpendicular to the crystal surface to intersect the branches of the dispersion surface. In the symmetrical Laue case this line will be parallel to the Brillouin zone boundary. Now let $\Upsilon^{(i)}$ be the distance between possible wavepoints $w^{(i)}$ and the point T and let s_g be the distance of reciprocal lattice point g from the Ewald sphere(both quantities are measured in the z direction i.e., normal to g). It can be seen from fig.1 that

Fig. 1

The dispersion surface and the Ewald sphere construction for high energy electrons. $w^{(1)}_T = \gamma^{(1)}$ and $w^{(2)}_T = \gamma^{(2)}$

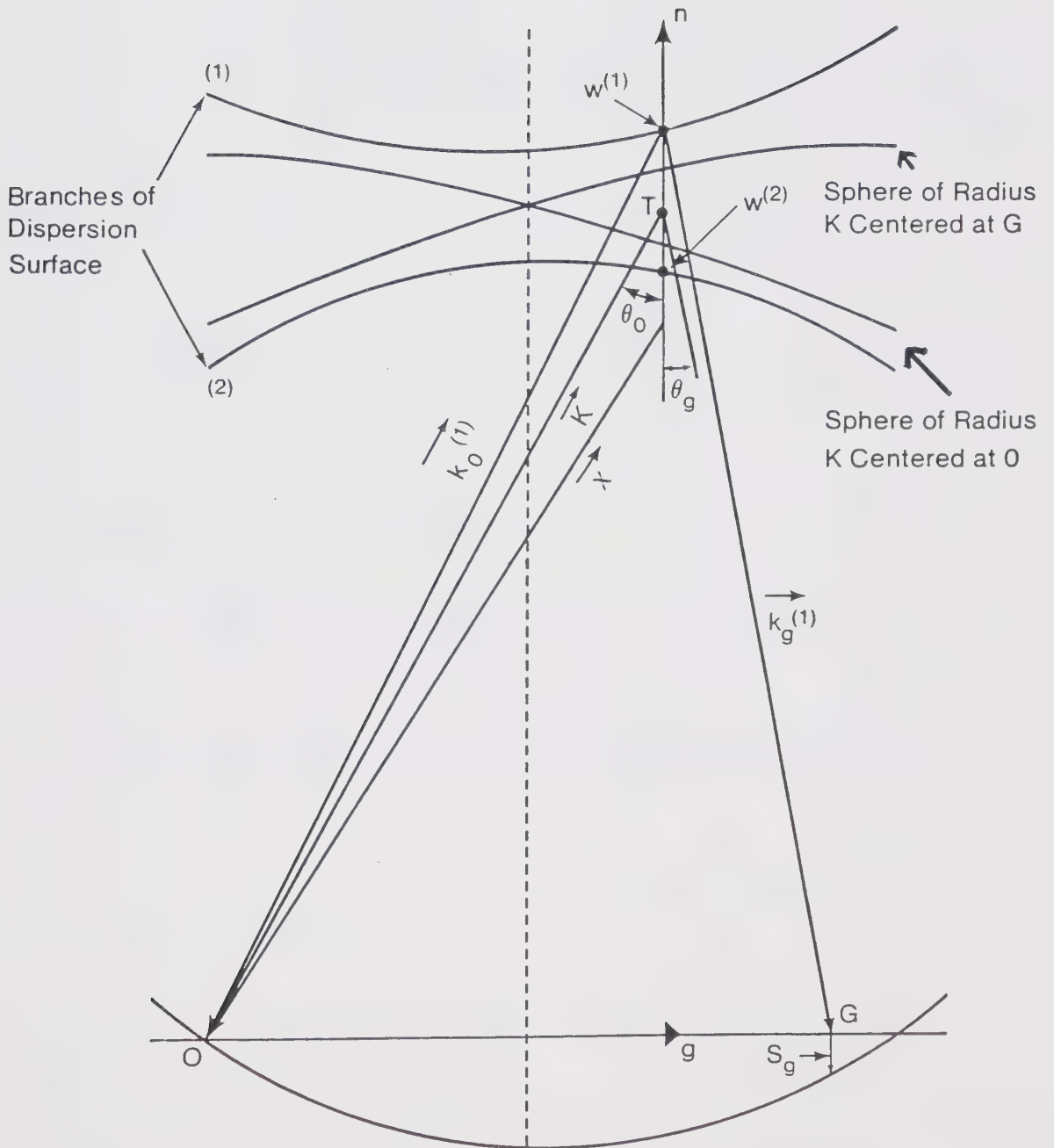


Figure 1

$$\begin{aligned}
K^2 - (\vec{K}_g^{(i)})^2 &\approx K^2 - (K - s_g \cos \theta_g + \Upsilon^{(i)} \cos \theta_g)^2 \\
&= K^2 - (K + (\Upsilon^{(i)} - s_g) \cos \theta_g)^2 \\
&= -2K(\Upsilon^{(i)} - s_g) \cos \theta_g [1 + \{(\Upsilon^{(i)} - s_g)/2K\} \cos \theta_g]
\end{aligned}
\tag{2.9}$$

If it is assumed that $K \gg g$ and $K \gg (\Upsilon^{(i)} - s_g)$ then

$$\cos \theta_g \approx 1 \tag{2.10}$$

and

$$\{(\Upsilon^{(i)} - s_g)/2K\} = 0 \tag{2.11}$$

Equation (2.9) then reduces to

$$K^2 - (\vec{K}_g^{(i)})^2 = -2K(\Upsilon^{(i)} - s_g) \tag{2.12}$$

and Bethe's equation (2.6) can be written in the eigenvalue form

$$\underline{A} \underline{C}^{(i)} = \Upsilon^{(i)} \underline{C}^{(i)} \tag{2.13}$$

Here $\underline{C}^{(i)}$ is a column vector whose elements $C_g^{(i)}$ are the Fourier coefficients in equation (1.1) (see chapter 1) and \underline{A} is a matrix with elements $A_{oo} = 0$, $A_{gg} = s_g$ and $A_{gh} = U_{g-h}/2K$ where $g \neq h$. The eigenvalue $\Upsilon^{(i)}$ is related to the z component of the Bloch wave vector $\vec{k}_o^{(i)}$ through the relation

$$(\vec{k}_0^{(i)})_z = K_z + \gamma^{(i)} \quad (2.14)$$

If N beams are considered the matrix \underline{A} will be an $N \times N$ matrix. Given such an input matrix, computer programs can be written to calculate the N eigenvalues and associated eigenvectors $[C_0^{(i)} \dots C_g^{(i)} \dots]$. By carrying out such matrix diagonalization procedures for a series of crystal orientations, it is possible to determine the shape of the different branches of the dispersion surface. In order to be able to refer to the different Bloch waves excited, it is convenient to label the Bloch waves and their corresponding branches of dispersion surface. The method generally adopted in the literature is to use the integer labels $i = 1, 2, 3, \dots$ in order of the decreasing values of $\gamma^{(i)}$ (Humphreys and Fisher, 1971).

2.2 The Calculation of Diffracted Beam Intensities in a Perfect Crystal

The total wave function $\Psi(\vec{r})$ of the high energy electron in the crystal can be written as a linear combination of all the Bloch waves excited, i.e.

$$\Psi(\vec{r}) = \sum_i \chi^{(i)} b^{(i)} = \sum_i \sum_g \chi^{(i)} C_g^{(i)} \exp\{2\pi i(\vec{k}^{(i)} + \vec{g}) \cdot \vec{r}\} \quad (2.15)$$

The coefficients $\chi^{(i)}$ in this expression are known as

excitation coefficients and determine the extent to which a particular Bloch wave is excited in the crystal. In order to calculate the diffracted beam intensity I_g , equation (2.15) is sorted out into components in the direction of \vec{g} . If these components are then multiplied by the phase term $\exp(-2\pi i \vec{K} \cdot \vec{r})$, the intensity of the beam g at depth z in the crystal is found to be

$$I_g(z) = | \Phi_g(z) |^2 = | \sum_i X^{(i)} C_g^{(i)} \exp(2\pi i Y^{(i)} z) |^2 \quad (2.16)$$

where $\Phi_g(z)$ is the amplitude of the beam g .

The excitation coefficients in equation (2.16) can be calculated from the boundary conditions at the top surface of the crystal, i.e.

$$\Phi_0(0) = 1, \quad \Phi_g(0) = 0 \quad (g \neq 0) \quad (2.17)$$

Equation (2.16) together with (2.17) gives

$$\underline{C} \underline{X} = \underline{u} \quad (2.18)$$

where \underline{C} is a square matrix having the elements $C_g^{(i)}$ in the g -th row and i -th column, \underline{X} is a column vector containing the excitation coefficients $X^{(i)}$ in the i -th row and \underline{u} is a column vector containing the diffracted beam amplitudes

1,0,0,... at the top surface of the crystal. The excitation coefficients in equation (2.16) can then be found by obtaining numerical solutions to the non homogenous set of linear equations (2.18). The effort to solve this set of equations can be greatly reduced when only elastic scattering is considered by noting that the \underline{A} matrix of equation (2.13) in this case is real and symmetric. Hence the matrix \underline{C} of normalized eigenvectors is orthogonal and $\underline{C}^{-1} = \underline{C}^T$, where \underline{C}^T is the transpose of \underline{C} . If equation 2.18 is multiplied from the left by \underline{C}^{-1} , then

$$\underline{X} = \underline{C}^T \underline{U} \quad (2.19)$$

and it can be immediately seen that the excitation coefficients $X^{(i)}$ are given by the elements in the first row of \underline{C} i.e.,

$$X^{(i)} = C_o^{(i)} \quad (2.20)$$

The expression for the diffracted beam intensity therefore becomes

$$I_g(z) = \left| \sum_i \phi_g^{(i)} \exp(2\pi i \Upsilon^{(i)} z) \right|^2 \quad (2.21)$$

where $\phi_g^{(i)} = C_o^{(i)} C_g^{(i)}$. Thus it can be seen that the contribution

of a particular Bloch wave to the g -th diffracted beam amplitude is determined by the magnitude of $\phi_g^{(i)}$ which is referred to as the excitation amplitude in this thesis.

2.2.1 Systematic and Non-systematic Reflections.

When a high energy electron beam is incident on a crystal it is generally found that a number of different sets of planes are close to satisfying their Bragg conditions. In forming conventional strong beam images the crystal is usually oriented so that only one low order diffracted beam is strongly excited. If this reflection has a reciprocal lattice vector \vec{g} , then all reflections corresponding to the vectors $n\vec{g}$ where n is an integer are called systematic reflections (Hoerni, 1956). Similarly those reflections which have reciprocal lattice vector, \vec{h} not colinear with \vec{g} are called non-systematic reflections. Whether a particular systematic reflection is termed systematic or non-systematic depends entirely upon the low-order diffracted beam being used for imaging purposes. Thus a reflection which is termed systematic in one situation may upon choosing a different low-order reflection for study, be termed non-systematic. This is illustrated in fig(2) which shows a computed electron diffraction pattern for a [310] orientation in a crystal with fcc structure. If the (002) reflection is the primary reflection being used in

Fig. 2

A computed diffraction pattern for $[310]$ orientation in a crystal with fcc structure.

$$\begin{pmatrix} 1 \\ 2 & -6 & -6 \end{pmatrix}$$

$$\begin{pmatrix} 1 \\ 1 & -3 & -5 \end{pmatrix}$$

$$\begin{pmatrix} 1 \\ 0 & 0 & -6 \end{pmatrix}$$

$$\begin{pmatrix} 1 \\ 2 & -6 & -4 \end{pmatrix}$$

$$\begin{pmatrix} 1 \\ 0 & 0 & -4 \end{pmatrix}$$

$$\begin{pmatrix} 1 \\ 1 & -3 & -3 \end{pmatrix}$$

$$\begin{pmatrix} 1 \\ -1 & 3 & -3 \end{pmatrix}$$

$$\begin{pmatrix} 1 \\ 2 & -6 & -2 \end{pmatrix}$$

$$\begin{pmatrix} 1 \\ 0 & 0 & -2 \end{pmatrix}$$

$$\begin{pmatrix} 1 \\ -2 & 6 & -2 \end{pmatrix}$$

$$\begin{pmatrix} 1 \\ 1 & -3 & -1 \end{pmatrix}$$

$$\begin{pmatrix} 1 \\ -1 & 3 & -1 \end{pmatrix}$$

$$\begin{pmatrix} 1 \\ 2 & -6 & 0 \end{pmatrix}$$

$$\begin{pmatrix} 1 \\ 1 \end{pmatrix}$$

$$\begin{pmatrix} 1 \\ -2 & 6 & 0 \end{pmatrix}$$

$$\begin{pmatrix} 1 \\ 1 & -3 & 1 \end{pmatrix}$$

$$\begin{pmatrix} 1 \\ -1 & 3 & 1 \end{pmatrix}$$

$$\begin{pmatrix} 1 \\ 2 & -6 & 2 \end{pmatrix}$$

$$\begin{pmatrix} 1 \\ 0 & 0 & 2 \end{pmatrix}$$

$$\begin{pmatrix} 1 \\ -2 & 6 & 2 \end{pmatrix}$$

$$\begin{pmatrix} 1 \\ 1 & -3 & 3 \end{pmatrix}$$

$$\begin{pmatrix} 1 \\ -1 & 3 & 3 \end{pmatrix}$$

$$\begin{pmatrix} 1 \\ 0 & 0 & 4 \end{pmatrix}$$

$$\begin{pmatrix} 1 \\ -2 & 6 & 4 \end{pmatrix}$$

$$\begin{pmatrix} 1 \\ 0 & 0 & 6 \end{pmatrix}$$

$$\begin{pmatrix} 1 \\ -1 & 3 & 5 \end{pmatrix}$$

$$\begin{pmatrix} 1 \\ -2 & 6 & 6 \end{pmatrix}$$

Figure 2

image formation, then the reflections (004) , (006) , $(00\bar{2})$, $(00\bar{4})$ and $(00\bar{6})$ are designated as systematic and all other reflections such as $(\bar{1}31)$, $(\bar{1}33)$ are designated as non-systematic.

2.3 Relativistic Corrections To The Dynamical Theory

The dynamical theory as it was originally formulated did not take into account relativistic effects. These effects have been considered by Fujiwara (1962), who developed a relativistic form of the dynamical theory using the Dirac wave equation. His results show that the non-relativistic theory can be corrected for relativistic effects by employing two simple corrections. These consist of replacing the non-relativistic wave length by the relativistically corrected one and multiplying the Fourier coefficient terms, $U_{\mathbf{g}}$ by a relativistic mass correction term

$$\beta = (1 - v^2/c^2)^{-1/2} \quad (2.23)$$

where v and c are the speeds of the electron and light respectively.

The imaginary part of the Fourier coefficients of the lattice potential $U'_{\mathbf{g}}$ (in case of inelastic scattering, see chapter 3) is relativistically corrected by multiplying $U'_{\mathbf{g}}$

by $v^{-1}\beta$ (Howie, 1962). The validity of these corrections has been confirmed experimentally by Hashimoto (1964), Dupouy et al. (1965) and Goringe et al. (1966).

CHAPTER 3

EFFECTS OF INELASTIC SCATTERING

3.1 Introduction

The theory described in the previous chapter does not take into account the effects of inelastic scattering. Electrons which are inelastically scattered outside the objective aperture do not contribute to the image and can therefore be considered to be absorbed (see fig.3). The effects of absorption are taken into account in the dynamical theory of electron diffraction by the addition of an imaginary part to the lattice potential (Dederichs (1972) or Kambe and Molière (1970)). There are several approaches which have been adopted in the literature to the solution of the Schrodinger equation including the imaginary potential (see chapter 1). The two approaches (i.e., standard method and exact method) which have been used in the present study, will be discussed in this chapter.

3.2 The Standard Theory for Taking Absorption into Account

In the standard method it is assumed that $V'(\vec{r}) \ll V(\vec{r})$, therefore permitting first order perturbation theory for the non-degenerate states to be used. The effect of the

Fig. 3

A schematic diagram showing the paths of electrons scattered inelastically outside the objective aperture (as for example AA').

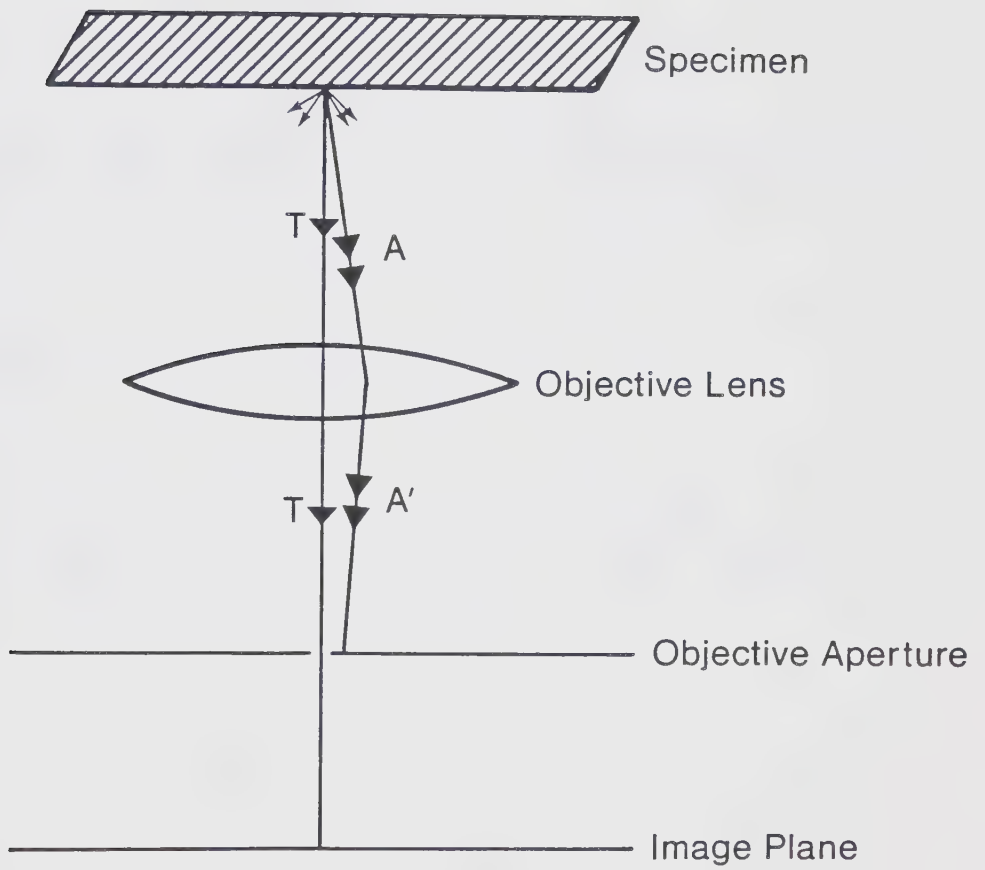


Figure 3

perturbation $iV'(\vec{r})$ is to change the energy of the Bloch wave by an amount $e\Delta E$ given by

$$e\Delta E = -i \int \langle b^{(i)} | V'(\vec{r}) | b^{(i)} \rangle d\tau \quad (3.1)$$

This energy change can be related to a change $\Delta k_z^{(i)}$ in the z component of the Bloch wave vector, i.e.,

$$\Delta k_z^{(i)} = -(me/h^2K) \Delta E = iq_z^{(i)} \quad (3.2)$$

where $q_z^{(i)}$ is the absorption coefficient of Bloch wave $b^{(i)}$. This coefficient can be calculated from the integral in equation 3.1 which gives the expression

$$q^{(i)} = (1/2K) \sum_g \sum_h C_g^{(i)} C_h^{(i)} U_{g-h}' \quad (3.3a)$$

In matrix form this equation becomes

$$q^{(i)} = (\underline{C}^{(i)})^T \underline{A}' \underline{C}^{(i)} \quad (3.3b)$$

where \underline{A}' is a matrix containing the elements $U_{g-h}'/2K$ in the g -th row and h -th column. It can be seen from equation 2.14 that the change $iq_z^{(i)}$ in $k_z^{(i)}$ will produce a similar change in $\gamma^{(i)}$. Accordingly, when the effects of inelastic scattering are included in the dynamical theory, the expression for the

diffracted beam intensity given in equation 2.16 becomes

$$I_g(z) = | \Phi_g(z) |^2 = | \sum_i C_o^{(i)} C_g^{(i)} \exp\{2\pi i(\gamma^{(i)} + iq^{(i)})z\} |^2 \quad (3.4)$$

By examining this relation it can be seen that the diffracted beam intensity is effectively attenuated or absorbed in the crystal due to the presence of the $\exp(-2\pi q^{(i)} z)$ terms. Calculations of the Bloch wave absorption parameters indicate that some Bloch waves are more highly absorbed than others. This has been explained by several authors (for example, Hashimoto, Howie and Whelan, 1962) in terms of Bloch wave channeling and gives rise to the well known effects of anomalous absorption.

3.2.1 Anomalous Absorption .

The differences between the absorption coefficients, $q^{(i)}$ gives rise to effects commonly referred to as anomalous absorption. In order to illustrate these effects, it is convenient to examine the variation of the diffracted beam intensity with thickness in the perfect wedge-shaped crystal. Consider first a situation where absorption is neglected and where it is assumed that there are only two Bloch waves with equal excitation amplitudes $C_o^{(i)} C_g^{(i)}$. In this case, diffracted beam intensity is found to vary sinusodially with crystal thickness as shown in fig(4a).

Fig. 4

The variation of diffracted beam intensity with thickness when (a) no absorption (b) normal absorption and (c) anomalous absorption is taken into account.

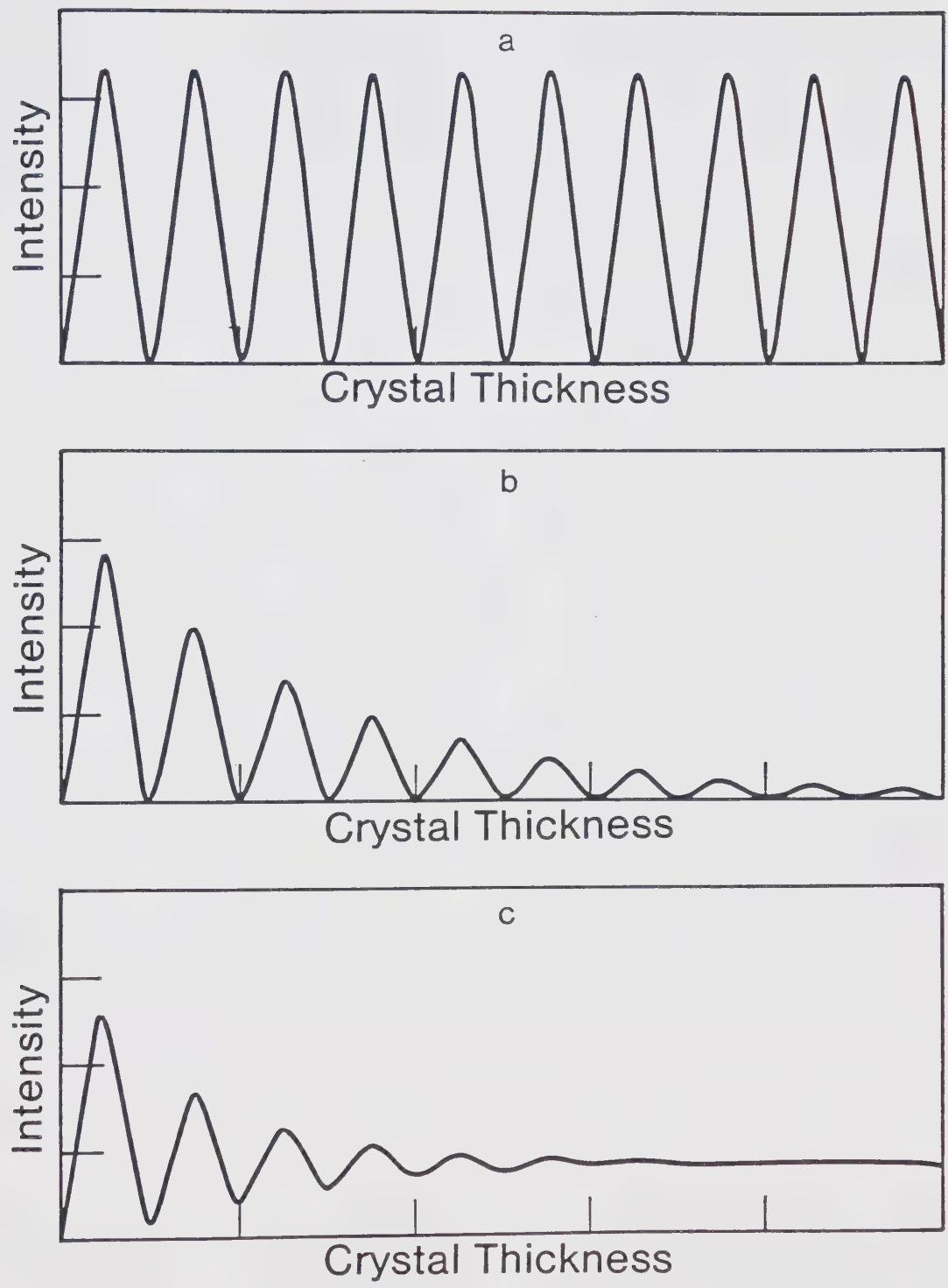


Figure 4

Fig.4(b) shows the same situation except that both important Bloch waves have been assumed to have equal absorption coefficients. It can be seen in fig.4(b) that the mean intensity decreases with increasing thickness but the sinusoidal variations are still present. This is termed as normal absorption and is characterized by the fact that the visibility or contrast of the fringes as measured by $(I_{\max} - I_{\min}) / (I_{\max} + I_{\min})$, does not change with depth in the crystal. Fig.4(c), on the other hand, shows the intensity profile obtained when one Bloch wave is absorbed much more strongly than the other. This profile illustrates the effect of anomalous absorption in a wedge-shaped crystal. In thicker regions the intensity variations have essentially disappeared due to the strong attenuation of one of the Bloch waves. However considerable diffracted beam intensity is still present due to the weakly absorbed beam. Besides having an important effect on intensity profiles in perfect crystals, anomalous absorption has also been found to lead to important effects in the images of crystal defects.

3.3 Exact method for Taking Absorption into Account

The exact method, based on the generalized perturbation theory, has been presented in detail in a paper by Andrew and Sheinin(1975), and therefore in this section this theory

is only summarized.

When the effects of absorption are taken into account by introducing an imaginary part to the lattice potential, the eigenvalue equation (2.13) becomes

$$(\underline{A} + i\underline{A}')\underline{C}'^{(n)} = \gamma'^{(n)}\underline{C}'^{(n)} \quad (3.5)$$

where $i\underline{A}'$ is a matrix in which the elements A'_{gh} are given by the relation $A'_{gh} = U'_{g-h}/2k$. The matrix $(\underline{A} + i\underline{A}')$ is no longer Hermitian and thus has complex eigenvalues and eigenvectors. The real eigenvalues and eigenvectors $\gamma^{(i)}$ and $\underline{C}^{(i)}$ in equation (2.13) have therefore been rewritten in equation (3.5) as the complex quantities $\gamma'^{(n)}$ and $\underline{C}'^{(n)}$ respectively. In the generalized perturbation theory approach to the solution of equation (3.5) the perturbed eigenvalues $\gamma'^{(n)}$ can be found without approximation by solving the eigenvalue equation

$$\underline{B}\underline{a}^{(n)} = \gamma'^{(n)}\underline{a}^{(n)} \quad (3.6)$$

where \underline{B} is a matrix which can be written as

$$B = \begin{bmatrix} \gamma^{(1)} + iq^{(1)} & iq^{(12)} & iq^{(13)} & \dots \\ iq^{(21)} & \gamma^{(2)} + iq^{(2)} & iq^{(23)} & \dots \\ iq^{(31)} & iq^{(32)} & \gamma^{(3)} + iq^{(3)} & \dots \\ \dots & \dots & \dots & \dots \end{bmatrix} \quad (3.6a)$$

The diagonal elements $\gamma^{(i)} + i q^{(i)}$ of \underline{B} are the sum of eigenvalues of the unperturbed equation 2.13 and absorption coefficients calculated by standard method, while the values of off-diagonal elements $q^{(ij)}$ are given by

$$\begin{aligned} q^{(ij)} &= 1/(2K) \langle b^{(i)} | U' | b^{(j)} \rangle \\ &= 1/(2K) \sum_g \sum_h C_g^{(i)} C_h^{(j)} U'_{g-h} \end{aligned} \quad (3.7a)$$

$$\text{and} \quad q^{(ii)} = q^{(i)} \quad (3.7b)$$

The off-diagonal elements $q^{(ij)}$ represent the mixing which occurs between a particular pair of unperturbed Bloch waves. The eigenvector $\underline{C}'^{(n)}$ can be found from the relation

$$\underline{C}'^{(n)} = \underline{C} \underline{a}^{(n)} \quad (3.8)$$

where \underline{C} is the matrix in which the columns are the eigenvectors of the unperturbed equation (2.13) and $\underline{a}^{(n)}$ is an eigenvector of equation (3.6). If \underline{C} is orthogonal and $\underline{a}^{(n)}$ is normalized, then $\underline{C}'^{(n)}$ will also be normalized.

3.3.1 Calculation of Diffracted Beam Intensities.

The expression for the diffracted beam intensity in the exact theory is similar to the one in the standard theory

(see equation 3.4) and can be written as

$$I_g(z) = \left| \sum_n X'^{(n)} C_g'^{(n)} \exp(2\pi i \Upsilon'^{(n)} z) \right|^2 \quad (3.9)$$

The eigenvalues $\Upsilon'^{(n)}$ in this equation can be found by diagonalizing the matrix \underline{B} and Bloch wave Fourier coefficients $C_g'^{(n)}$ can be found by substituting the eigenvectors of \underline{A} and \underline{B} matrices into equation (3.8) . The excitation coefficients $X'^{(n)}$ can be found by numerical solution of the non-homogenous system of linear equations (2.18) .

CHAPTER 4

THEORETICAL CALCULATIONS

4.1 Introduction

The work presented in this thesis relies extensively on numerical calculations based on the standard and exact theories presented in the last two chapters. It is therefore important to indicate the procedure used to calculate and diagonalize the matrices \underline{A} (see equation 2.13) and \underline{B} (see equation 3.6) and then to calculate absorption coefficients $q^{(i)}$, excitation amplitudes $|\phi_{220}^{(i)}|$ and diffracted beam intensities. These procedures will be discussed in this chapter. Since the work presented in this thesis involves Bloch wave degeneracies, it is also important to indicate the diffraction conditions at which the degeneracies are obtained. This will also be discussed in this chapter.

4.2 Setting up the \underline{A} matrix

4.2.1 Calculation of the Diagonal Elements of \underline{A} Matrix.

The diagonal elements of the \underline{A} matrix (see equation 2.13, chapter 2) can be expressed in terms of the deviation

Fig. 5

The intersection of the Ewald sphere with the zero order Laue zone. The orientation is specified by the tie point method. The point L is the perpendicular projection of the centre of the Ewald sphere (tie-point) on the zero order Laue plane.

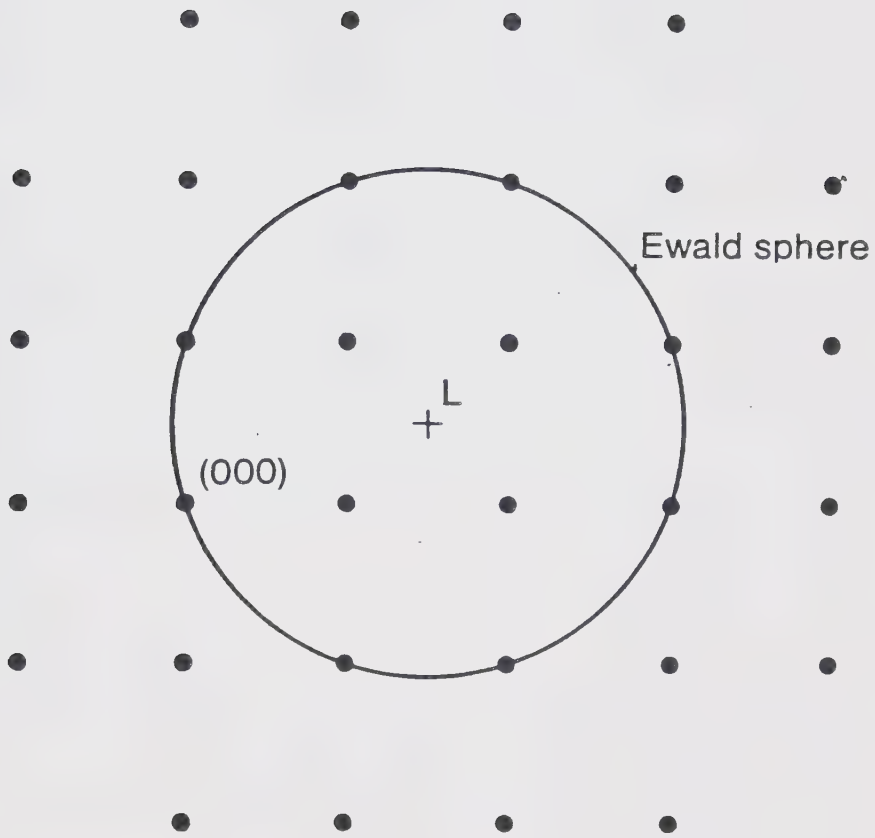


Figure 5

Fig. 6

The dispersion surface and the Ewald sphere construction showing parameters required for calculation of diagonal elements of the A matrix.

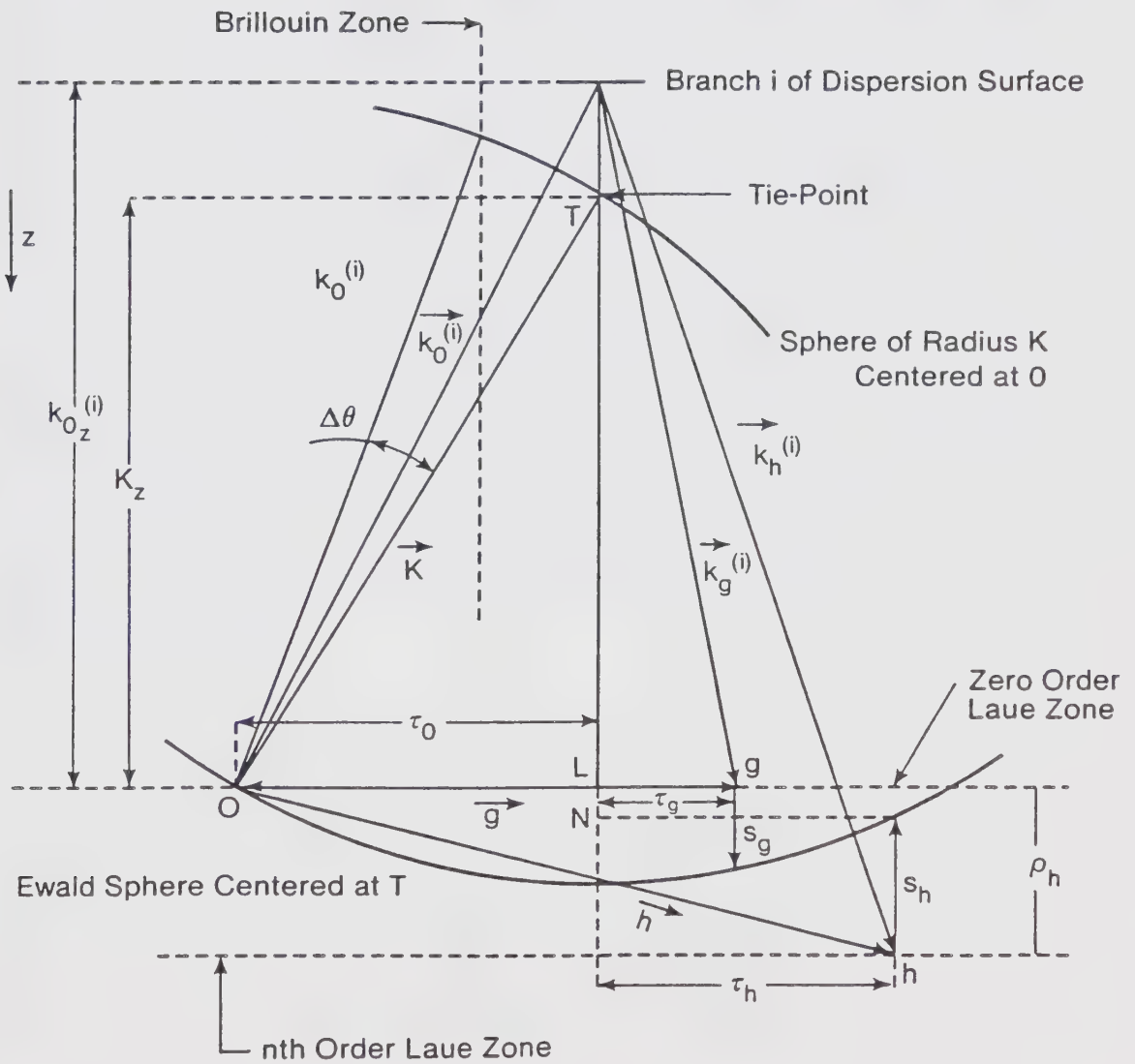


Figure 6

parameter s_h where s_h is defined to be the distance from the reciprocal lattice point h to the Ewald sphere in the z -direction (see fig.6). When the position of the Ewald sphere is specified using the tie-point method (in this method the crystal orientation is specified by the co-ordinates of the point L which is the perpendicular projection of the tie point in to the zero order Laue plane (see fig.5 and fig.6)), then values of s_h can be calculated with the aid of Fig(6). In this figure, the symmetrical Laue case has been assumed and the point L is the projection of the tie-point T on the zero order Laue plane. It can be seen that the value of s_h for some reflection h in the n th order Laue zone is

$$\begin{aligned} s_h &= LN - \rho_h = TN - TL - \rho_h \\ &= (K^2 - \tau_h^2)^{1/2} - (K^2 - \tau_0^2)^{1/2} - \rho_h \end{aligned} \quad (4.1)$$

Using a Taylor series expansion of the two square roots and retaining terms up to second order, gives

$$s_h \approx (1/2K)(\tau_0^2 - \tau_h^2) + (1/8K^3)(\tau_h^4 - \tau_0^4) \quad (4.2)$$

This method of calculating the diagonal elements of the \underline{A} matrix will be referred to as the s -value method.

It is of interest to note that if only the first order term of equation 4.2 is retained, the s-values for reflection g in the zero order zone becomes,

$$s_g \approx (1/2K)(\tau_o^2 - \tau_g^2) \quad (4.3a)$$

$$= (1/2K)(\tau_o + \tau_g)(\tau_o - \tau_g)$$

$$= (1/2K)g(\tau_o + \tau_o - \tau_o - \tau_g)$$

$$= (1/K)g(\tau_o - g/2)$$

$$\approx g\Delta\theta \quad (4.3b)$$

where $\Delta\theta$ is defined in fig.(6). This first order approximation is used by many authors(see for example Head et.al., 1973)

4.2.2 The Calculation Of The Off-Diagonal Elements Of The A Matrix.

The off-diagonal elements of the A matrix(see section 2.2) for a crystal composed of only one type of atom are given by

$$U_{g-h} = \frac{\beta}{\pi V_e} F_{g-h} f_e (\sin\theta_{g-h} / \lambda) \exp(-B|\vec{g} - \vec{h}|^2/4) \quad (4.4)$$

where, β is the relativistic mass correction factor for the incident electrons, V is the volume of the unit cell in the crystal, F_{g-h} is the kinematical structure factor,

$f(\sin\theta_{q-h} / \lambda)$ is the atomic scattering factor for electrons and B is the Debye Waller factor for the material considered. The scattering factors used in this thesis were calculated by Doyle and Turner(1968) using relativistic Hartree-Fock atomic wave fuctions. Values for the Debye-Waller B factor are also given in literature(Ibers and Vainshtein, 1962).

4.3 Setting up the B matrix

The diagonal elements of the B matrix(see equation 3.6) are obtained by first diagonalizing the real matrix A (see section 4.4). The absorption coefficients of the standard theory (see section 4.8) and the off-diagonal elements q can then be calculated from the equation (3.7a).

4.4 Diagonalization of matrices A and B

In order to obtain $\gamma^{(i)}$ and $C^{(i)}$, the matrix A (see equation 2.13), which is real and symmetric, was diagonalized by using the subroutines EHOUSS, EQRT2S, EHOBKS in IMSL subroutine package(1979). It should be noted that there are other subroutines in the IMSL(1979) which could have been used. A comparison of all the routines was carried out and it was found that the subroutines used in the present study require the least computing time and the results are more accurate than those obtained by using other

subroutines(Cann 1973)

To calculate $\gamma^{(n)}$ and $\underline{C}^{(n)}$ the complex matrix \underline{B} (see equation 3.6) was diagonalized by using the IMSL(1979) subroutine EIGCC.

4.5 Reflections chosen in the calculations

In this thesis three beam calculations have been carried out with the three reflections (000), (220), ($\bar{1}33$). In a comparison of experimental results with many beam and three beam dynamical theory, Cann and Sheinin(1974) found that there are three important Bloch waves when ($\bar{1}33$) reflection is close to its Bragg condition. In order to verify that no other reflections have a significant effect on the final result, both three and multi-beam calculations of Bloch wave parameters were carried out for different materials which have been considered in this thesis. Good agreement was obtained between the results of both sets of calculations, indicating that in this case the simple three beam approximation is adequate for predicting the effects of a Bloch wave degeneracy in the presence of non-systematic reflections. In order to determine the effect of higher order non-systematic reflections a study has been carried out with the higher order non-systematic reflection ($\bar{1}37$).

One question which arises when performing the multi-beam calculations is how many reflections should be

Fig. 7

A computed diffraction pattern for a $[334]$ orientation in a crystal with fcc structure showing the 11 reflections which were considered in the many beam calculations.



Figure 7

included. In view of the fact that the computing time required for a particular calculation increases considerably with the number of reflections taken into account, it was necessary to develop a criterion which selects only those beams which are relevant to the results obtained. The procedure used in the present work was to increase the number of reflections included until a stage was reached when the addition of further reflections did not change the intensity profile or the values of Bloch wave parameters $C_g^{(i)}$, $\gamma^{(i)}$ and $q^{(i)}$ in any significant way. In this way eleven reflections were considered for the multi-beam calculations (see fig.7).

4.6 Diffraction conditions for which the Bloch wave degeneracies are obtained

The conditions for the occurrence of a Bloch wave degeneracy in the presence of a non-systematic reflection h (Cann and Sheinin 1974; Gjønnes and Hoier 1971) are given by

$$s_g = \left(\frac{U_g}{U_h} \right) \left(\frac{U_{g-h}^2 - U_h^2}{2K U_{g-h}} \right) \quad (4.5)$$

$$s_h = \left(\frac{U_h}{U_g} \right) \left(\frac{U_{g-h}^2 - U_g^2}{2K U_{g-h}} \right) \quad (4.6)$$

where s_g and s_h are the deviation parameters of reflection g and h (see section 4.2.1) and U_g and U_h are parameters related to the Fourier coefficients of the lattice potential (see equation 2.1, chapter 2). For the particular case of (220) and ($\bar{1}33$) the expressions (4.5) and (4.6) reduce to

$$s_{220} = 0 \quad (4.5a)$$

$$s_{\bar{1}33} = \frac{U_{\bar{1}33}^2 - U_{220}^2}{2K U_{220}} \quad (4.6a)$$

and similarly for the case of (000), (220), ($\bar{1}37$)

$$s_{220} = 0 \quad (4.5b)$$

$$s_{\bar{1}37} = \frac{U_{\bar{1}37}^2 - U_{220}^2}{2K U_{220}} \quad (4.6b)$$

In these particular cases two Bloch waves will be degenerate only when (220) reflection is in its Bragg condition and deviation parameter of ($\bar{1}33$) and ($\bar{1}37$) are given by equations 4.6a and 4.6b. This is illustrated in fig.8 which shows that Bloch waves 2 and 3 are degenerate at $\Delta\theta_{\bar{1}33} = -0.05\theta_{\bar{1}33}$ ($\Delta\theta_{\bar{1}33}$ is the deviation of ($\bar{1}33$) reflection from its Bragg condition, given in fractions of $\theta_{\bar{1}33}$ the ($\bar{1}33$) Bragg angle). This value of $\Delta\theta_{\bar{1}33}$ as taken from the curves

Fig. 8

The variation of $\gamma^{(i)}$ ($i = 1, 2, 3$) with $\Delta\theta_{\bar{1}33}$ as given by a three beam calculation including (000), (220), and ($\bar{1}33$) reflections. $\Delta\theta_{220} = 0.0$.

Fig. 9

The variation of $\gamma^{(i)}$ ($i = 1, 2, 3$) with $\Delta\theta_{\bar{1}33}$ as given by a three beam calculation including the (000), (220), and ($\bar{1}33$) reflections. $\Delta\theta_{220} = -0.1\theta_{220}$.

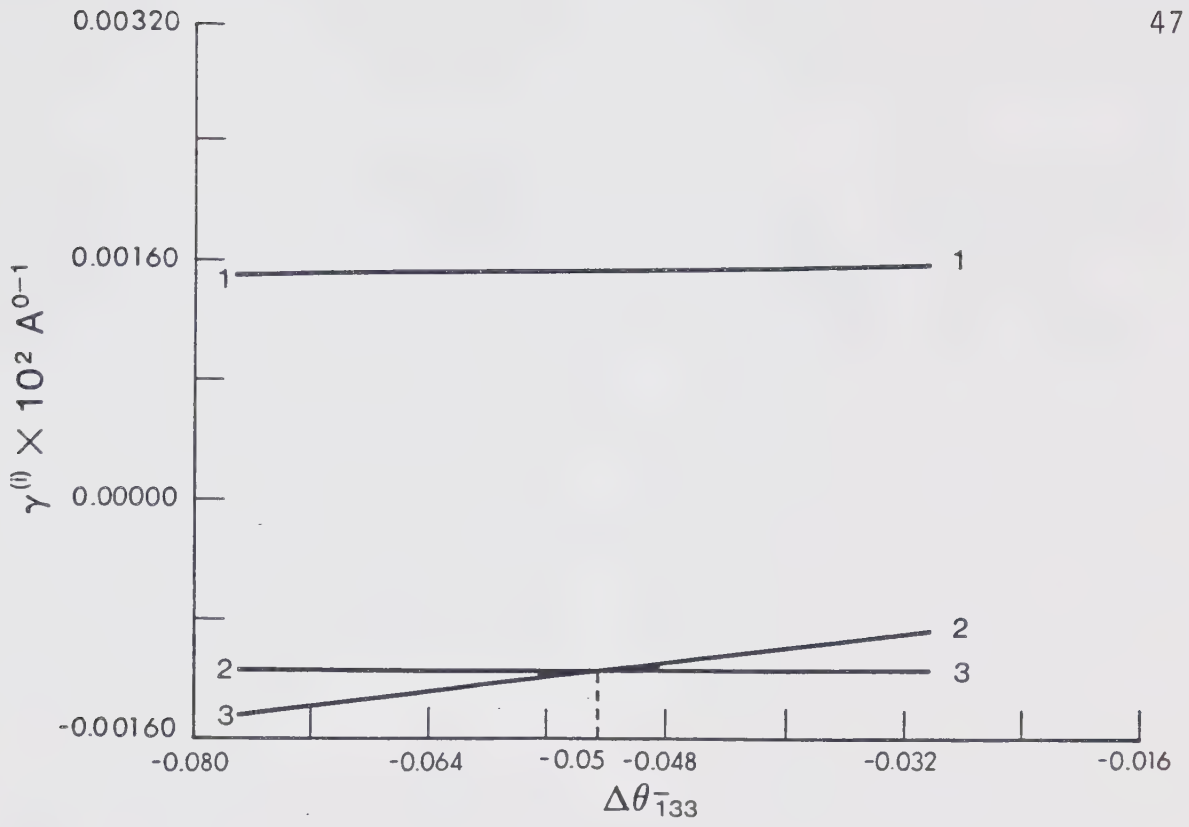


Figure 8

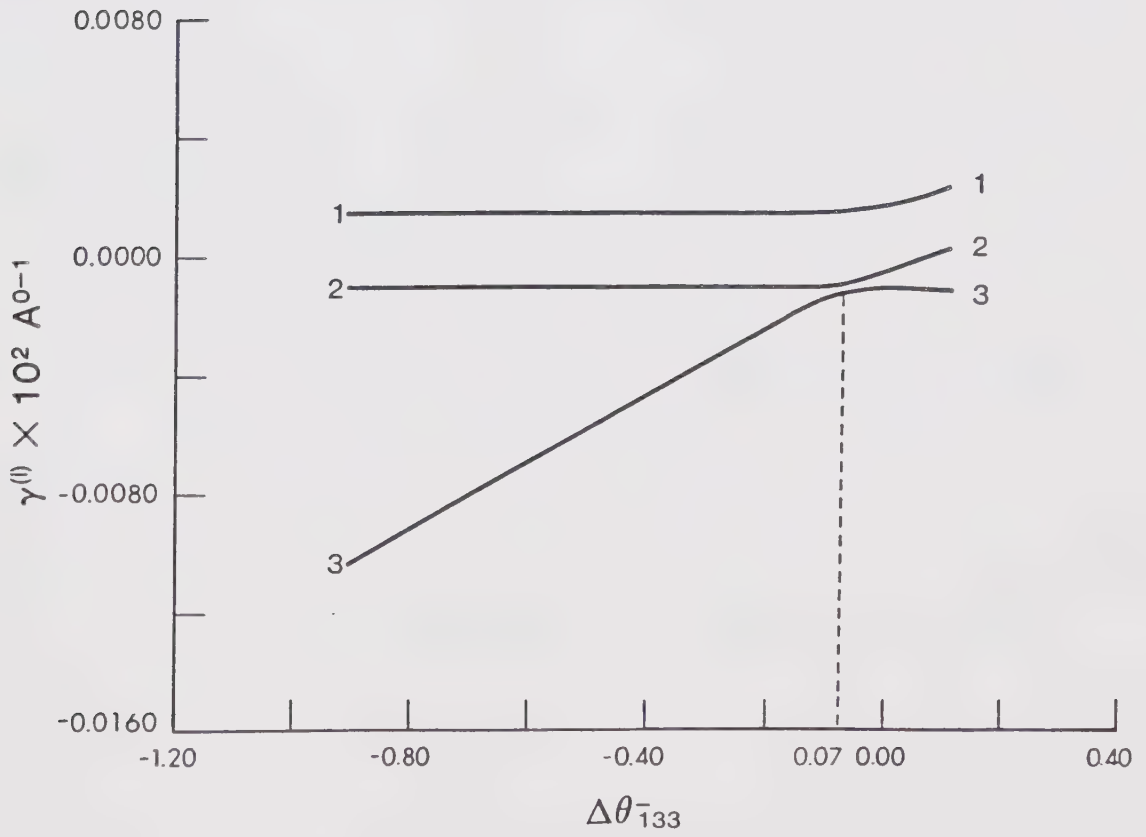


Figure 9

corresponds to a deviation parameter $s_{\bar{1}33} = -0.107 \times 10^{-3} \text{ \AA}^\circ$ in agreement with the value obtained from equation (4.6a).

When the (220) reflection is not in the Bragg condition a degeneracy does not occur. However when $\Delta\theta_{220}$ is small, Bloch waves 2 and 3 are nearly degenerate, a condition which will be referred as quasi-degeneracy. This is illustrated in fig.9, which shows the quasi-degeneracy at $\Delta\theta_{\bar{1}33} = -0.07\theta_{\bar{1}33}$ ($s_{\bar{1}33} = -0.2 \times 10^{-3} \text{ \AA}^\circ$) and $\Delta\theta_{220} = -0.1\theta_{220}$ ($s_{220} = -0.56 \times 10^{-6} \text{ \AA}^\circ$).

4.7 Calculation of Absorption coefficients, Excitation amplitude and Diffracted beam intensity using the Standard method

The absorption coefficients $q^{(i)}$ were calculated by using equation (3.3a) (see chapter 3). In order to carry out this calculation the imaginary component of the lattice potential U_g' must first be obtained (see equation 4.7). This was done by using the ratios U_g'/U_g given by Humphreys and Hirsch (1968). The excitation amplitude $|\phi_g^{(i)}|$ as given by $C_o^{(i)} C_g^{(i)}$ (see equation 2.21), can be obtained from the eigenvectors of matrix \underline{A} (see section 4.4). The diffracted beam intensity I_g was obtained from equation 3.4 (see chapter 3).

4.8 Calculation of Absorption coefficients, Excitation amplitude and Diffracted beam Intensity using the exact method

The absorption coefficients $q^{(i)}$ in exact method were obtained by diagonalizing the complex matrix \underline{B} where the imaginary part of the eigenvalue gives the absorption coefficient (see chapter 3, section 3.3). The excitation amplitudes $|\phi_g^{(i)}|$, given by $X^{(i)} C_g^{(i)}$, where the Bloch wave Fourier coefficients $C_g^{(i)}$ found by diagonalizing the matrix B (see section (4.4) and the excitation coefficients $X^{(i)}$ found by solving the linear equation (2.18) (in this case \underline{C} , \underline{X} and \underline{u} are complex) using the IMSL (1979) subroutine LEQ2C. The diffracted beam intensities were obtained by writing a program based on equation (3.4) and in which $X^{(i)}$, $C_g^{(i)}$, $\gamma^{(i)}$ and $q^{(i)}$ were calculated by using exact method.

CHAPTER 5

RESULTS AND DISCUSSION

5.1 Introduction

The Bloch wave absorption coefficients $q^{(i)}$ and excitation amplitudes $|\phi_{220}^{(i)}|$ have been calculated as a function of $\Delta\theta_{\bar{1}33}$ ($\Delta\theta_{\bar{1}33}$ is the deviation of the reflection ($\bar{1}33$) from its Bragg condition) by using the standard and exact methods. Calculations have been carried out for both three beam (including (000), (220), and ($\bar{1}33$) reflections) and eleven beam cases (see fig.7). The intensity profiles (i.e., diffracted beam intensity plotted as function of crystal depth) at the point where Bloch waves 2 and 3 are degenerate ($s_{220} = 0$) or quasi-degenerate ($|s_{220}|$ is close to zero) have also been obtained by using both methods. Calculations have been carried out for three materials including Si, Cu and Au and a comparison of all the calculations based on the standard method with those based on exact method has been made. In the plots of $q^{(i)}$ and $|\phi_{220}^{(i)}|$ as a function of $\Delta\theta_{\bar{1}33}$, Bloch wave one has not been included. The principle reason for this is that the values of $q^{(i)}$ and $|\phi_{220}^{(i)}|$ are not effected by degeneracy and therefore both the standard and the exact methods give the

same results for this Bloch wave. A study has also been carried out to determine the effects of a higher order non-systematic reflection ($\bar{1}37$). Results of all these studies will be presented in the subsequent sections of this chapter.

5.2 A Comparison of Absorption coefficients, Excitation amplitudes and Diffracted beam intensities obtained with Standard and Exact methods.

5.2.1 The case of degenerate diffraction conditions.

It was indicated in the previous chapter (see section 4.6) that in the presence of the non-systematic reflection ($\bar{1}33$), a Bloch wave degeneracy occurs when the (220) reflection is in its Bragg condition. The first calculations to be presented are for the medium atomic number material copper at an accelerating voltage 100Kv. Figures 10(a,b) and 11(a,b) show the variation of $|\phi_{220}^{(i)}|$ and $q^{(i)}$ with $\Delta\theta_{\bar{1}33}$ obtained by using standard and exact methods respectively. From these figures it can be seen that there is no significant difference between the values of $|\phi_{220}^{(i)}|$ or $q^{(i)}$ obtained from either method. A point of interest which should be noted, however is that there is an interchange in the values of $|\phi_{220}^{(i)}|$ and $q^{(i)}$ for Bloch waves 2 and 3 which occurs at the point of degeneracy. The value of $\Delta\theta_{\bar{1}33}$ at the point where the interchange occurs has

Fig. 10(a,b)

The variation of excitation amplitude $|\phi_{220}^{(i)}|$ ($i = 2,3$) with $\Delta\theta_{133}$ for Cu, at $\Delta\theta_{220} = 0$ calculated by (a) the standard and (b) the exact methods.

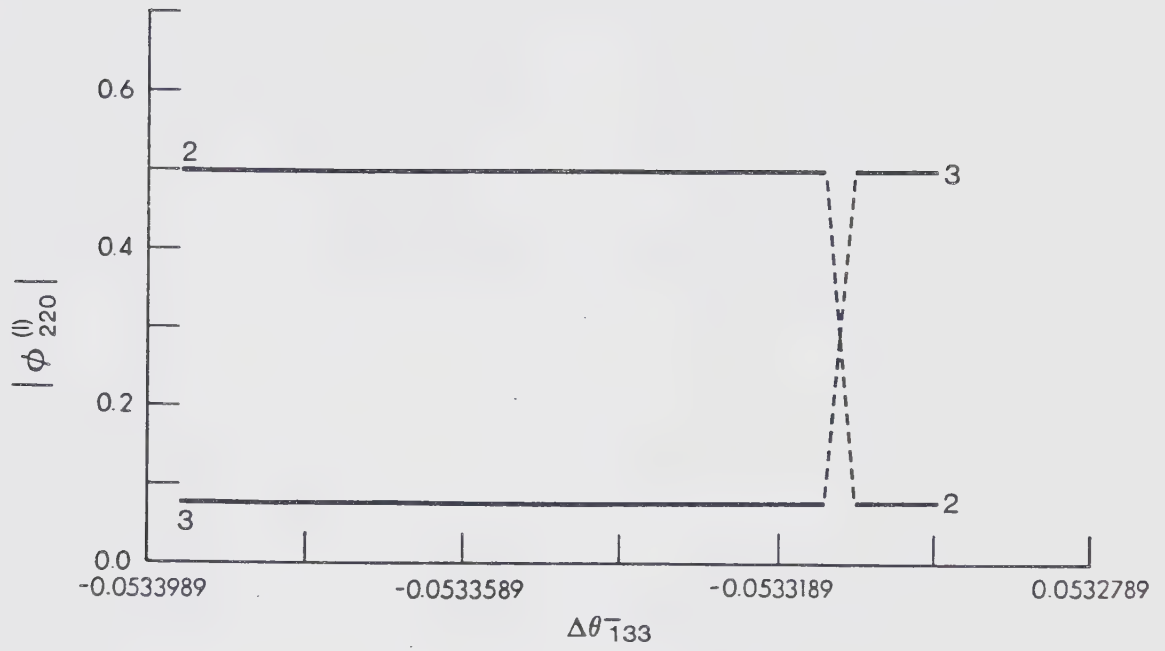


Figure 10 (a)

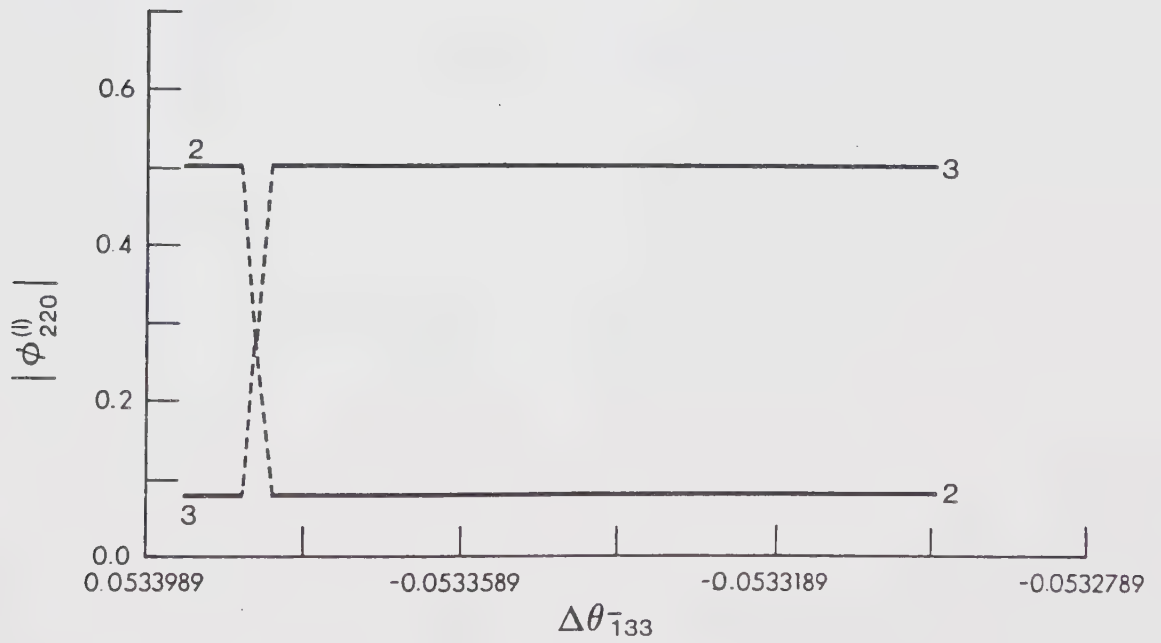


Figure 10 (b)

Fig. 11(a,b)

The variation of Bloch wave absorption coefficients $q^{(i)}$ with $\Delta\theta_{133}$ for Cu, at $\Delta\theta_{220} = 0$, calculated by using (a) the standard and (b) the exact methods.

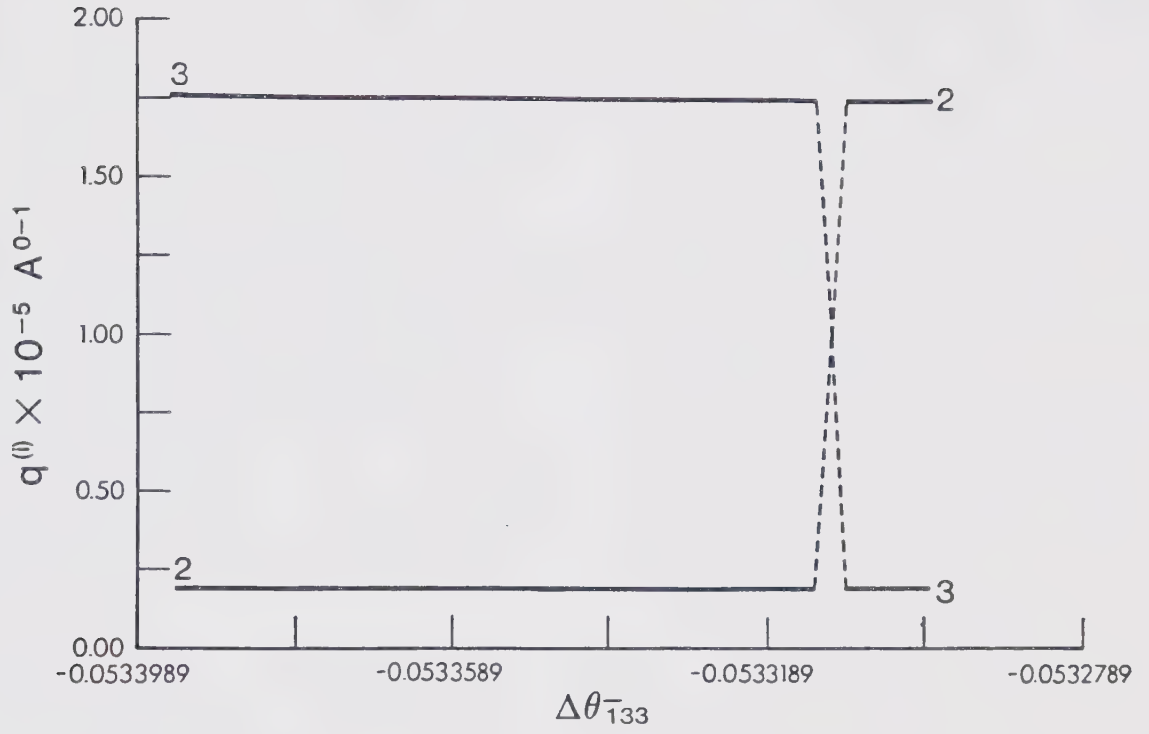


Figure 11 (a)

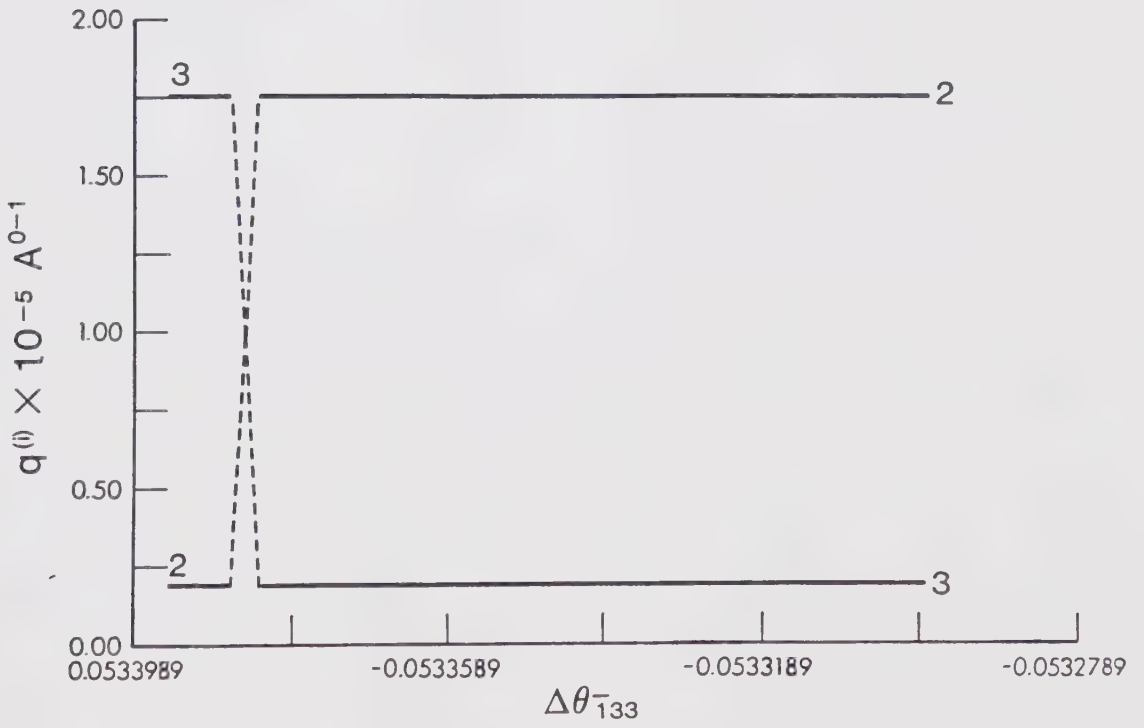


Figure 11 (b)

TABLE 1

Percentage differences in the absorption coefficients and diffracted beam intensities calculated by using both standard and exact methods at the point where Bloch waves 2 and 3 are degenerate. Three beam calculations were used and the results shown are for silicon, copper and gold.

$$\Delta\theta_{220} = 0 \quad \text{Accelerating voltage} = 100 \text{ kv.}$$

Crystal thickness for Cu and Au = 1500 \AA

Crystal thickness for Si = $15,000 \text{ \AA}$

	$\left \frac{q_s^{(i)} - q_E^{(i)}}{q_s^{(i)}} \right \times 100$		$\left \frac{I_s - I_E}{I_s} \right \times 100$
	i = 2	i = 3	
Si	0.002	0.0	0.04
Cu	0.24	0.0	0.12
Au	1.02	0.0	0.18

different values for the two methods. However, because this interchange occurs at a particular value of $\Delta\theta_{133}$, the values of the parameters in equation (3.4) (see chapter 3) for $i = 2, 3$ remain unaffected on passing through the degeneracy point. As a result there should be no significant difference in the intensity profiles obtained by the two methods in this case, as indicated by the data in table(1).

Similar calculations have also been carried out for gold and silicon. The results obtained with these two elements were found to be similar in character to those obtained for copper (see table 1)

5.2.2 Results in the case of quasi-degenerate diffraction conditions.

In section 4.6 (chapter 4) it was indicated that when there is a small deviation of (220) reflection from its Bragg condition Bloch waves 2 and 3 can be considered to be quasi-degenerate (see fig. 9). In this thesis a study of the quasi-degenerate state has been carried out for a value of $\Delta\theta_{220} = -0.0001\theta_{220}$.

The results obtained for copper are shown in Fig.12(a,b) and Fig.(13). Figures 12(a,b) show the variation of $q^{(i)}$ and $|\phi_{220}^{(i)}|$ ($i = 2, 3$) with $\Delta\theta_{133}$ obtained from both standard and exact theories. It can be seen from

Fig. 12(a,b)

The variation of (a) excitation amplitude $|\phi_{220}^{(i)}|$ ($i = 2,3$) and (b) the variation of $q^{(i)}$ ($i = 2,3$) with $\Delta\theta_{133}$.

Calculations were carried out for Cu using both exact and standard methods, at a value of $\Delta\theta_{220} = -0.0001\theta_{220}$.

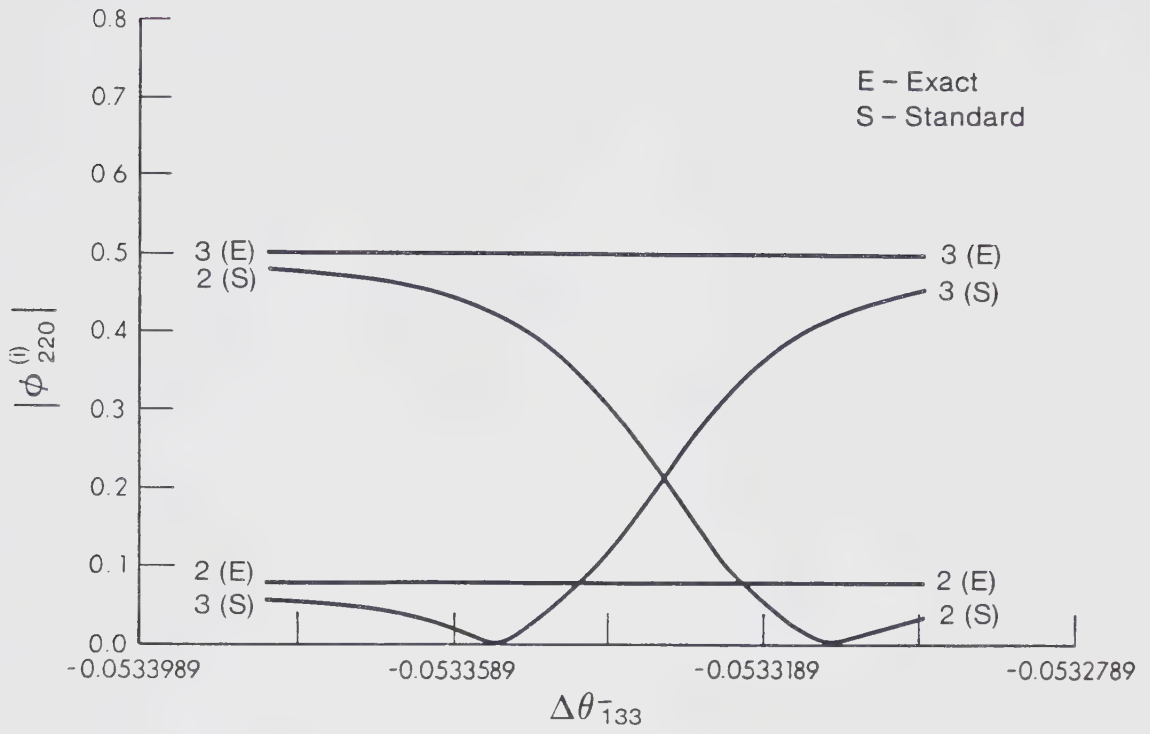


Figure 12 (a)

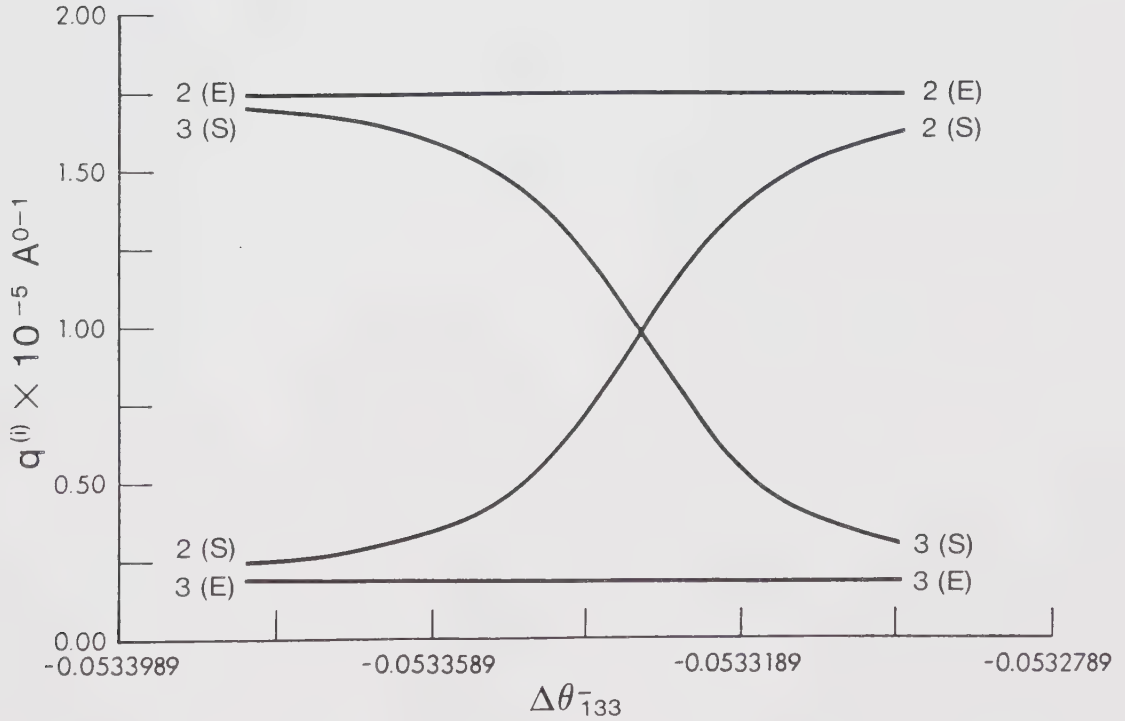


Figure 12 (b)

Fig. 13

The variation of diffracted beam intensity with crystal thickness for Cu obtained by using the standard and exact methods. Calculations were carried out at the point where Bloch waves 2 and 3 are quasi-degenerate, i.e. at $\Delta\theta_{133} = -0.05\theta_{133}$ and $\Delta\theta_{220} = -0.0001\theta_{220}$.

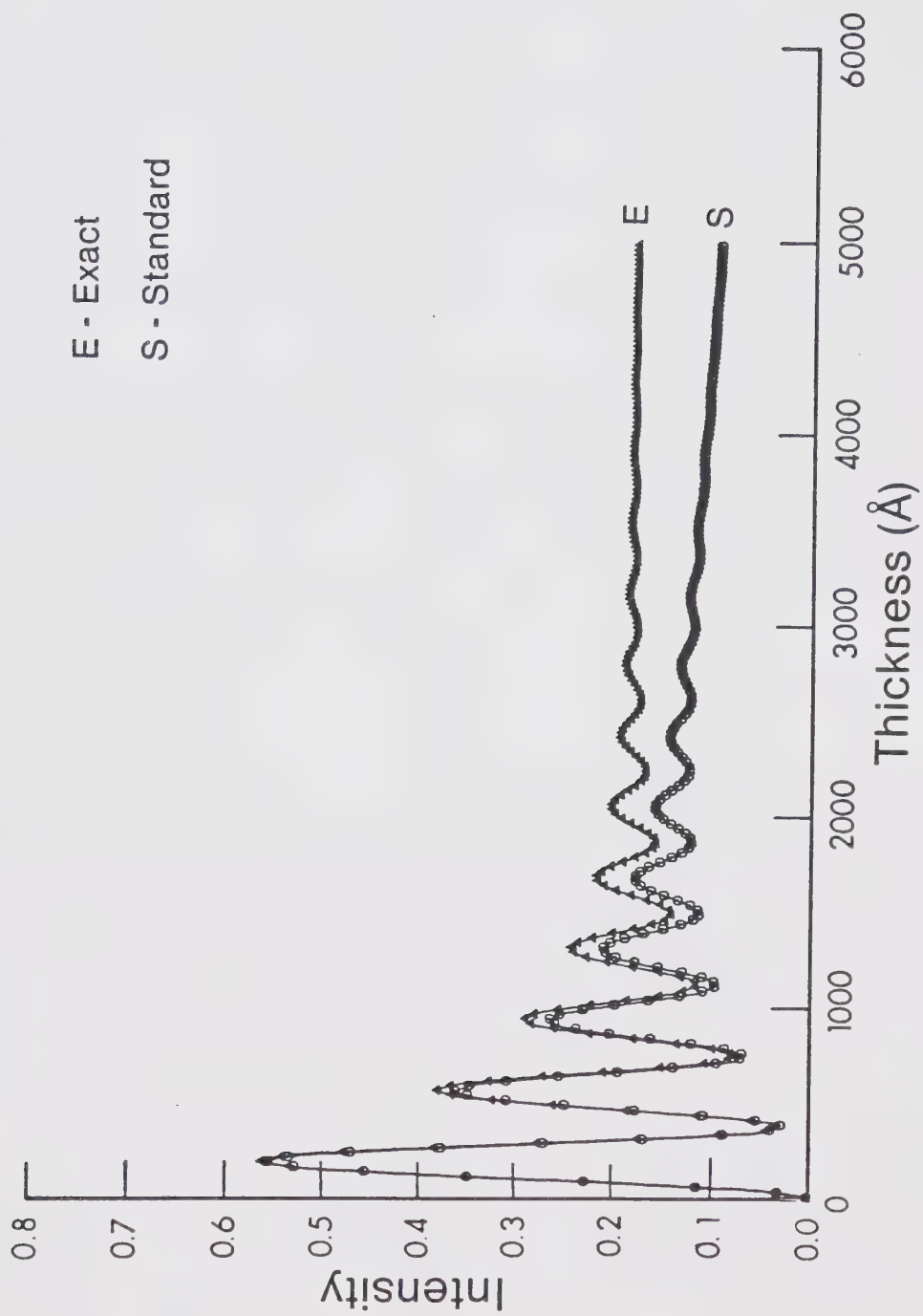


Figure 13

these Figures that in the case of the standard method the interchange in the values of $q^{(i)}$ or $|\phi_{220}^{(i)}|$ occur over a range of values of $\Delta\theta_{133}$ (i.e., the interchange is continuous). In the case of the exact method the interchange is similar in character to that obtained in the case of degenerate diffraction conditions(not shown in fig.12). From fig.12(a,b) it can be seen that at the point where Bloch waves 2 and 3 are quasi-degenerate, i.e., at $\Delta\theta_{133} = -0.05333\theta_{133}$, the standard method gives $q^{(2)} = q^{(3)}$ and $|\phi_{220}^{(2)}| = |\phi_{220}^{(3)}|$, whereas the exact method values are quite different. As a result it would be expected that the intensity profiles obtained with the two methods would be quite different as shown in figure (13). It should be noted from this figure that there is no appreciable change in the overall shape of the intensity profiles obtained from the two theories and the peak to peak spacing is not noticeably altered. The two theories, however, give significant differences in diffracted beam intensity.

Similar calculations have been carried out for silicon and gold. The results obtained were found to be similar in character to those for Cu as illustrated in figures (14), (15) and table (2).

Fig. 14

The variation of diffracted beam intensity with crystal thickness for Si obtained by using the standard and exact methods. Calculations were carried out at the point where Bloch waves 2 and 3 are quasi-degenerate, i.e. at $\Delta\theta_{\bar{1}33} = -0.05\theta_{\bar{1}33}$ and $\Delta\theta_{220} = -0.0001\theta_{220}$.

Fig. 15

The variation of diffracted beam intensity with crystal thickness for Au obtained by using the standard and exact methods. Calculations were carried out at the point where Bloch waves 2 and 3 are quasi-degenerate, i.e. at $\Delta\theta_{\bar{1}33} = -0.115\theta_{\bar{1}33}$ and $\Delta\theta_{220} = -0.0001\theta_{220}$.

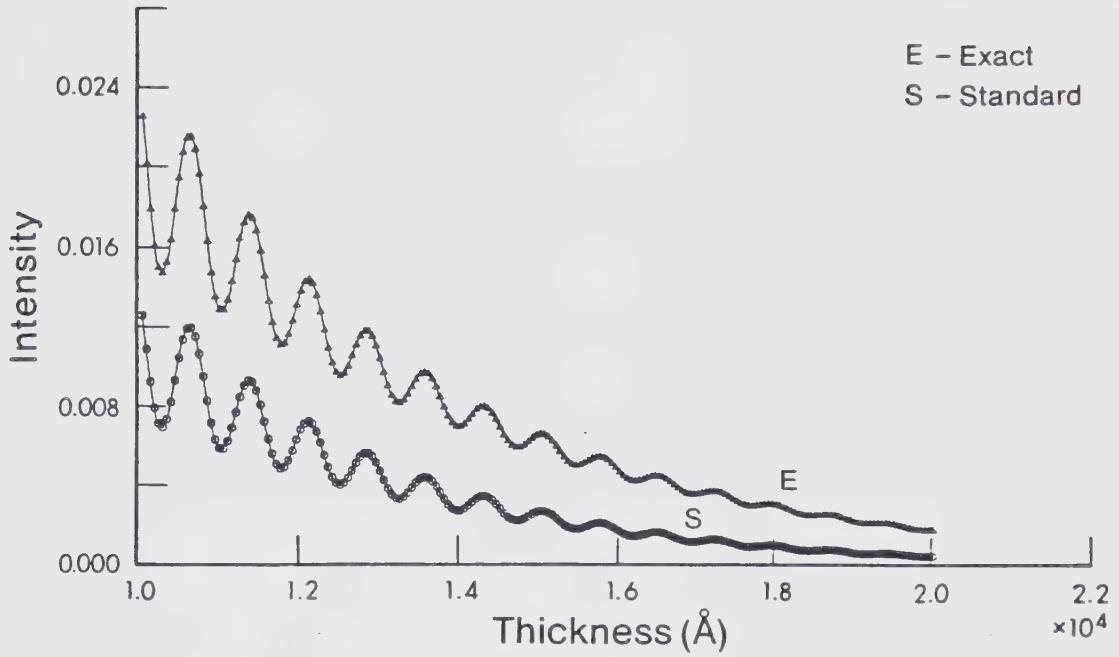


Figure 14

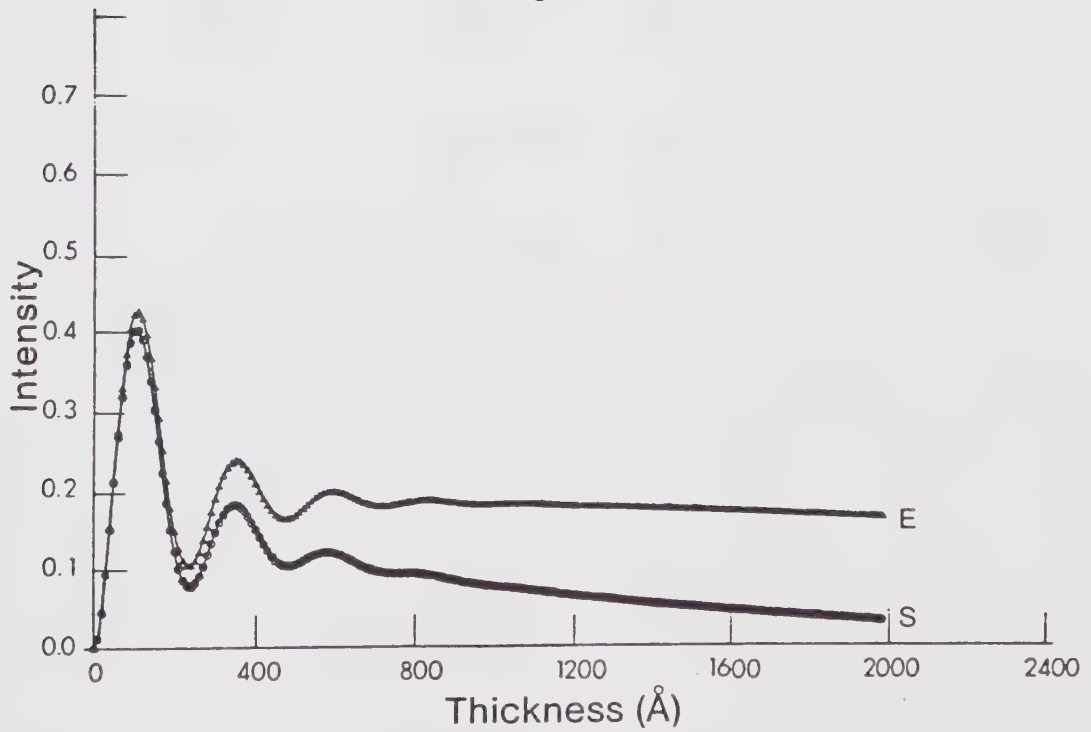


Figure 15

TABLE 2

Percentage differences in absorption coefficients and diffracted beam intensities calculated by using standard and exact method at the point where Bloch waves 2 and 3 are quasi-degenerate. 3 beam and 11 beam calculations were used and the results shown are for Si, Cu and Au.

$$\Delta\theta_{220} = -0.0001\theta_{220} \quad \text{Accelerating voltage} = 100\text{kv}$$

Crystal thickness for Cu and Au = 1500 \AA

Crystal thickness for Si = $15,000 \text{ \AA}$

	$\left \frac{q_s^{(i)} - q_E^{(i)}}{q_s^{(i)}} \right \times 100$				$\left \frac{I_s - I_E}{I_s} \right \times 100$	
	i = 2		i = 3			
	3 beam	11 beam	3 beam	11 beam	3 beam	11 beam
Si	18.66	24.65	18.70	24.92	60.58	70.21
Cu	71.57	88.30	79.35	82.72	19.90	21.50
Au	83.05	98.50	80.46	98.90	71.33	85.89

Fig. 16(a)

The variation of the Bloch wave absorption coefficients $q^{(i)}$ with $\Delta\theta_{133}$ for Cu at $\Delta\theta_{220} = -0.0001\theta_{220}$, calculated by using both standard and exact methods. 11 beams were taken into account in the calculations.

Fig. 16(b)

The variation of diffracted beam intensity with crystal thickness for Cu obtained by using the standard and exact methods. Calculations were carried out at the point where Bloch waves 2 and 3 are quasi-degenerate, i.e. at $\Delta\theta_{133} = -0.03\theta_{133}$ and $\Delta\theta_{220} = -0.0001\theta_{220}$. 11 beams were taken into account in the calculations.

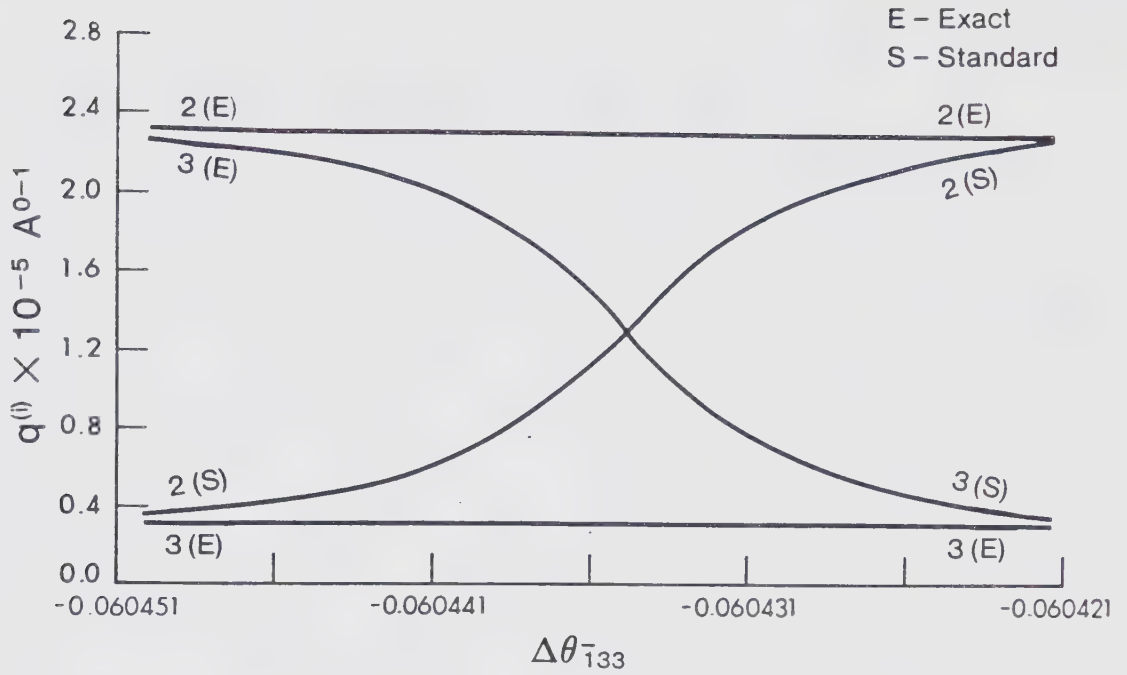


Figure 16 (a)

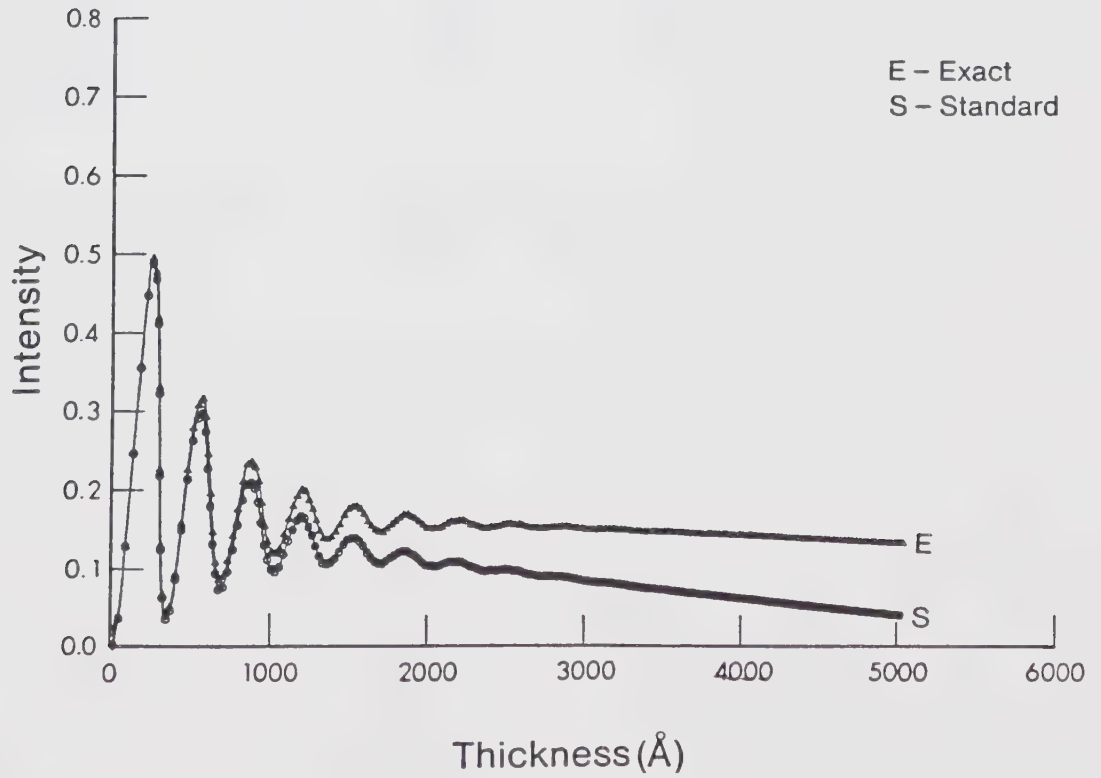


Figure 16 (b)

5.2.3 Results in the multi-beam case.

Multi-beam calculations have also been performed in order to find out if the three beam approximation is adequate. Calculations have been carried out for the three elements (i.e, Cu, Au and Si) for quasi-degenerate diffraction conditions (i.e, when $\Delta\theta_{220} = -0.0001\theta_{220}$). Eleven reflections have been considered (see section 4.7) for these calculations. It has been found that the results obtained are similar in character to those obtained in three beam case, as illustrated by the results obtained for Cu are shown in fig.16(a,b) and figures (12,13) (see page 48,49) and table(2).

5.2.4 Effects of higher order non-systematic reflection.

A study has been carried out to see if the effects found in the previous sections are affected by the order of the non-systematic reflection. The reflection considered for this study is ($\bar{1}37$) and calculations have been carried out for both Si and Cu. Both degenerate ($\Delta\theta_{220} = 0$) and quasi-degenerate ($\Delta\theta_{220} = -0.0001\theta_{220}$) diffraction conditions have been considered. The first calculations have been carried out for Cu. It has been found that in case of degenerate diffraction conditions, the results are similar in character to those obtained for ($\bar{1}33$) reflection

Fig. 17(a)

The variation of the Bloch wave absorption coefficients $q^{(i)}$ with $\Delta\theta_{137}$ for Cu. Calculations were carried out by using both standard and exact methods at a value of $\Delta\theta_{220} = -0.0001\theta_{220}$.

Fig. 17(b)

The variation of diffracted beam intensity with crystal thickness for Cu obtained by using the standard and exact methods. Calculations were carried out at the point where Bloch waves 2 and 3 are quasi-degenerate, i.e. at $\Delta\theta_{137} = -0.03\theta_{137}$ and $\Delta\theta_{220} = -0.0001\theta_{220}$.

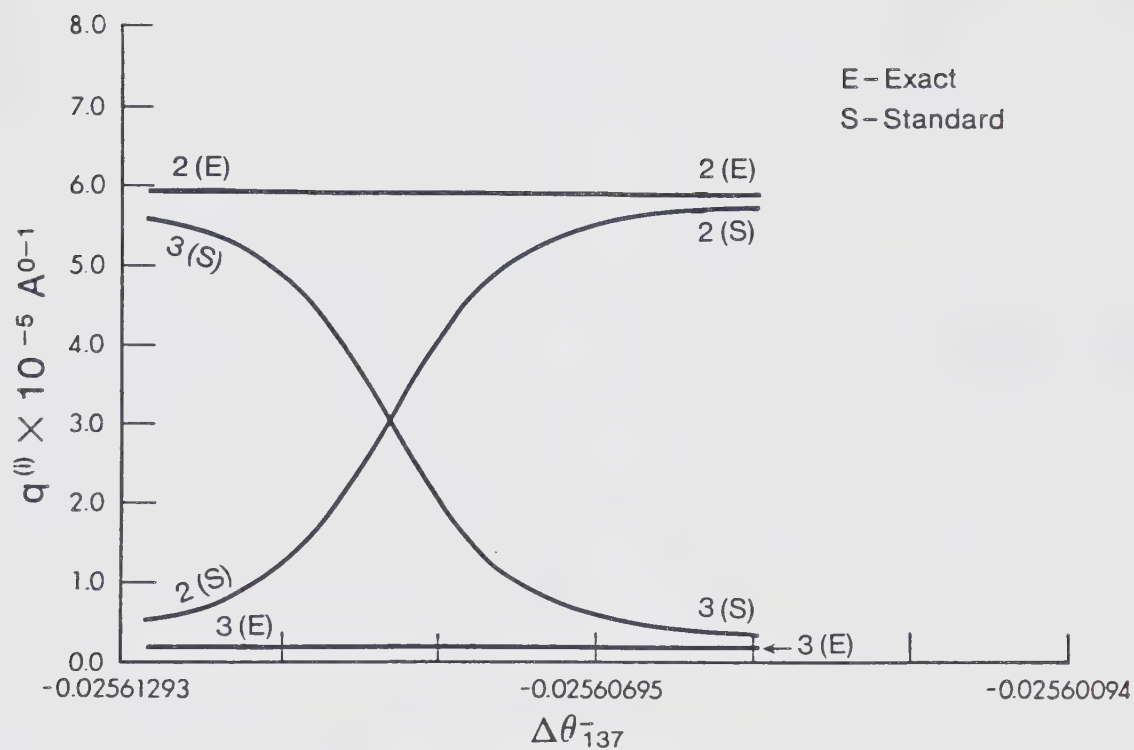


Figure 17 (a)

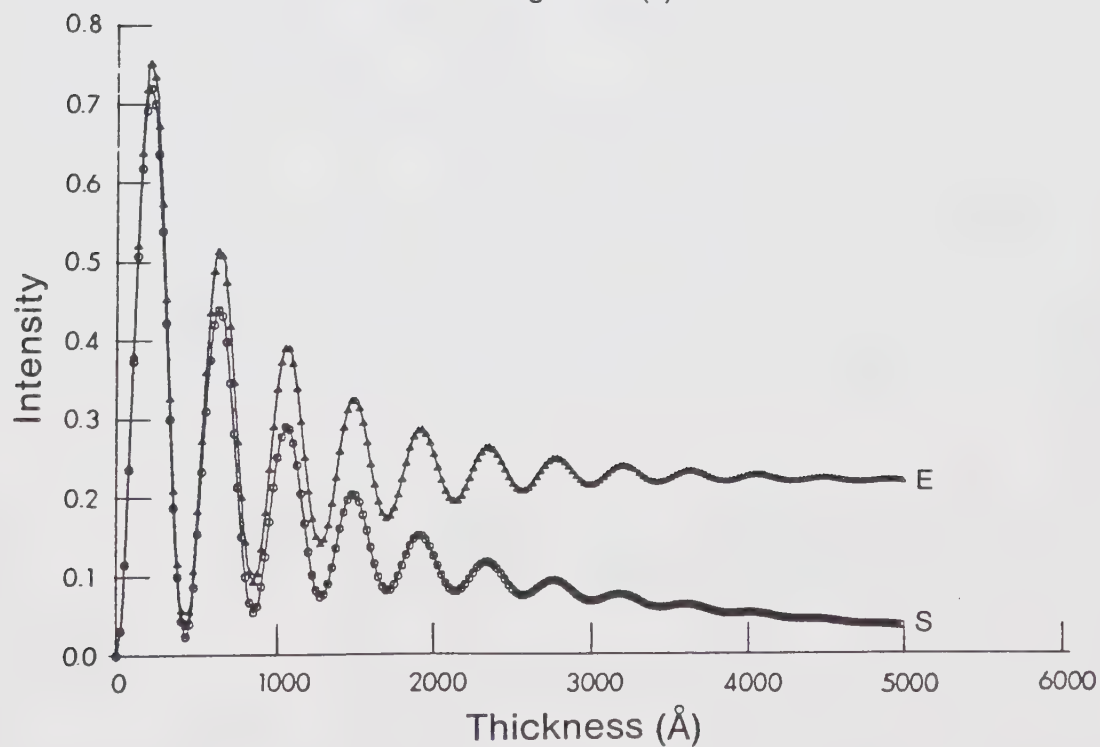


Figure 17 (b)

TABLE 3

Percentage differences in absorption coefficient and diffracted beam intensities calculated by using standard and exact method at the point where Bloch waves 2 and 3 are degenerate and quasi-degenerate. 3 beam calculations were used including (000), (220) and ($\bar{1}37$) reflections and the results shown are for Si and Cu.

Crystal thickness for Cu = 1500 Å

Crystal thickness for Si = 15,000 Å

Accelerating voltage = 100kv

$\Delta\theta_{220}$	Element	$\left \frac{q_s^{(i)} - q_E^{(i)}}{q_s^{(i)}} \right \times 100$		$\left \frac{I_E - I_S}{I_S} \right \times 100$
		i = 2	i = 3	
0.0001 θ_{220}	Si	0.002	0.0	0.05
	Cu	0.39	0.0	0.30
-0.0001 θ_{220}	Si	22.39	33.01	67.14
	Cu	83.30	92.70	37.33

and therefore no significant differences were found in the results obtained with standard and exact methods (see table(3)). In the case of quasi-degenerate diffraction conditions, however, significant differences have been found in the results obtained with the two methods as shown in figures 17(a,b) and table(3). Similar calculations have been carried out for Si. The results obtained are similar in character to those obtained for Cu (see table 3).

It is of interest to compare the results obtained for the low order reflection ($\bar{1}33$) with those of higher order reflection ($\bar{1}37$). In order to carry out this comparison percentage differences in diffracted beam intensity have been calculated for different crystal thickness as a constant value of $\Delta\theta_{220}$ (see table 4). Calculations of diffracted beam intensity using the two theories have also been carried out for different values of $\Delta\theta_{220}$ as a constant crystal thickness (see table 5). It can be seen from the table(4) and table(5) that the differences in the results obtained by using both methods are greater in the case of ($\bar{1}37$) reflection than in the case of ($\bar{1}33$) reflection. The reason for this will be discussed in the next section.

TABLE 4

Percentage differences in diffracted beam intensities calculated by using standard and exact method at the point where Bloch waves 2 and 3 are quasi-degenerate. 3 beam calculations were used and the results shown are for Cu.

$$\Delta\theta_{220} = -0.0001\theta_{220}$$

$$\text{Accelerating voltage} = 100\text{kv}$$

Crystal Thickness In $\text{\AA}^\circ \longrightarrow$	$\left \frac{I_s - I_E}{I_s} \right \times 100$		
	2000	3000	4000
($\bar{1}33$)	27.94	47.50	65.87
($\bar{1}37$)	102.15	240.12	320.56

TABLE 5

Percentage differences in diffracted beam intensities calculated by using standard and exact method at the point where Bloch waves 2 and 3 are quasi-degenerate. 3 beam calculations were used and the results shown are for Cu.

Accelerating voltage = 100kv and Crystal thickness for Cu = 10000 Å

$\Delta\theta_{220}$	$\left \frac{I_s - I_E}{I_s} \right \times 100$	
	($\bar{1}33$)	($\bar{1}37$)
-0.0 θ_{220}	0.16	0.30
-0.00001 θ_{220}	30.34	98.74
-0.0001 θ_{220}	32.34	98.76
-0.001 θ_{220}	32.45	98.78
-0.01 θ_{220}	41.87	98.85
-0.05 θ_{220}	33.61	89.73
-0.1 θ_{220}	1.87	46.56
-0.2 θ_{220}	1.13	36.56
-0.3 θ_{220}	0.3	10.34

5.3 Discussion

The results described in section 5.2.1 showed that for degenerate diffraction conditions i.e., when the systematic reflection is in its Bragg condition, there are no significant differences in the absorption coefficients and diffracted beam intensities obtained from the standard and exact methods. The results described in sections 5.2.2 and 5.2.4 on the other hand showed that for quasi-degenerate diffraction conditions i.e., when the systematic reflection is close to its Bragg condition there are significant differences in the results obtained from the two methods. The manner in which these differences arise differ in three important respects. The first of these can be seen from the numerical calculations in table(5) (see page 59) which show that the differences occur over a range of values of

$\Delta\theta_{220}$. This table shows that the significant differences in the diffracted beam intensities obtained when the two methods for calculating the absorption coefficient were used, occur over a range of values of $\Delta\theta_{220}$ from about $-0.00001\theta_{220}$ to $-0.1\theta_{220}$ in case of (133) reflection.

The second important feature of the results presented in this thesis can be seen by comparing the results for different materials as shown in table(2) (see page 52). These results show that the differences in absorption coefficients and diffracted beam intensities obtained from

the two methods are greater in the case of Au than in the case of Cu, which indicates that the errors increase with increasing atomic number. From tables (1), (2) and (3) (see pages 46, 52 and 56) it can be seen that the results obtained for diamond cubic crystal (Si) are similar in character to those obtained for the face centered cubic crystals (Cu and Au).

The third important feature of the results presented in this thesis can be seen by comparing the results obtained for low and higher order non-systematic reflections in tables (4) and (5) (see page 58, 59). These results show that the differences obtained from using the two methods increase significantly with order of the non-systematic reflection. The underlying reasons for this behaviour will be discussed in the next section.

5.3.1 A discussion of the effect of order of the non-systematic reflections on absorption coefficients when the systematic reflection is close to its Bragg condition.

The results described in section 5.2.4 and tables (4) and (5) (see pages 58,59) showed that the differences in the results obtained from the two methods for calculating absorption coefficients are greater in case of $(\bar{1}37)$ reflection than for $(\bar{1}33)$ reflection. This can be explained in terms of the characteristics of the \underline{B} matrix. The most

TABLE 6

B matrices for three beam calculations in which (a) (000), (220), ($\bar{1}33$) and (b) (000), (220), ($\bar{1}37$) reflections are included .

$$\Delta\theta_{220} = -0.0001\theta_{220} \quad \text{Accelerating voltage} = 100 \text{ kv}$$

(a) \underline{B} matrix ($\times 10^{-3} \text{ \AA}^{-1}$)	Change in the imaginary part of the diagonal elements ($q^{(i)}$) after diagonalization ($\times 10^{-6} \text{ \AA}^{-1}$)
$\begin{array}{ccc} 1.55+0.23i & -0.03i & 0.032i \\ -0.03i & -1.14+0.009i & -0.0078i \\ 0.032i & -0.0078i & -1.14+0.01i \end{array}$	$\begin{array}{c} 0.055 \\ 7.24 \\ 7.30 \end{array}$
(b) \underline{B} matrix ($\times 10^{-3} \text{ \AA}^{-1}$)	Change in the imaginary part of the diagonal elements ($q^{(i)}$) after diagonalization ($\times 10^{-6} \text{ \AA}^{-1}$)
$\begin{array}{ccc} 1.20+0.18i & -0.04i & -0.037i \\ -0.04i & -1.14+0.035i & 0.028i \\ -0.37i & 0.028i & -1.14+0.03i \end{array}$	$\begin{array}{c} 0.074 \\ 24.050 \\ 24.120 \end{array}$

important point to note is that the amount by which the standard theory eigenvalues ($\Upsilon^{(i)} + iq^{(i)}$), which are equal to the diagonal elements of the \underline{B} matrix, are modified by the off-diagonal elements depends on the value of these elements as well as the differences between the diagonal elements (Andrew and Sheinin 1975). It can be seen from table(6) that the differences between the diagonal elements of the B matrix are less for ($\bar{1}37$) reflection than in the case of ($\bar{1}33$) reflection. It is clear therefore that the difference in the absorption coefficients obtained from standard and exact(diagonalizing the \underline{B} matrix) methods should be greater in case of ($\bar{1}37$) reflection than in the case of ($\bar{1}33$) reflection as has in fact been found (see the right column of table 6).

The reason for the decrease in difference between the eigenvalues ($\Upsilon^{(i)}$) with increasing order of non-systematic reflection was explained by Cann(1973). In a determination of extinction distance in the presence of higher order non-systematic reflections Cann found that the minimum difference between the eigenvalues is equal to $U_h/\sqrt{2}k$. This shows that the difference is directly proportional to Fourier coefficient of the lattice potential of the non-systematic reflection involved. Since these coefficients in general decrease in magnitude with increasing order of non-systematic reflection, the decrease

in differences between the eigenvalues with increasing order of the non-systematic reflection is explained.

5.4 Conclusions

The original purpose of the work undertaken in this thesis was to determine the errors obtained from using the standard theory to calculate absorption coefficient in the dynamical theory of electron diffraction for the case where Bloch wave degeneracies occur due to the presence of non-systematic reflections. In order to carry out such investigation a comparison of the calculations based on standard theory with those based on exact theory has been carried out.

In attempting to assess the significance of the results in this thesis the first point to consider is the importance of taking non-systematic reflections into account in diffraction contrast calculations. In the past most calculations of diffraction contrast have been based on either the two-beam dynamical theory or the multi-beam theory taking systematic reflections into account. In practice, the assumption that only systematic reflections are present is open to question since non-systematic reflections must to some extent be excited. In the calculations of diffraction contrast involving these

reflections the electron microscopist is confronted with problem of choosing either standard method or the exact method to calculate absorption coefficients.

In this thesis it has been shown that there are no significant errors obtained in using the standard theory to calculate absorption coefficient when diffraction conditions are such that a Bloch wave degeneracy is obtained in the presence of non-systematic reflection, significant errors, however, are obtained in the case of quasi-degenerate diffraction conditions. It is important to appreciate that in practice it may be very difficult for the electron microscopist to judge, from the diffraction pattern, whether degenerate or quasi-degenerate diffraction conditions obtain. In this situation significant errors may be obtained by using standard method to calculate absorption coefficient and therefore it is important to use the exact method. It has also been indicated in this thesis that the errors obtained by using the standard method increase with increasing atomic number and with increasing order of the non-systematic reflection. It is therefore clear that there are many possible situations for which the exact theory should be used when non-systematic reflections are taken into account in the calculation of diffraction contrast.

One final point should be noted. The above conclusions are based on three beam calculation and therefore only a

single non-systematic reflection is taken into account. In practice there may be a number of non-systematic reflections excited which may have significant effect on the results obtained. Since each non-systematic reflection can give rise to a degeneracy, it is possible that the errors described in this thesis may be considerably greater in practice. Further investigation is of course required to substantiate this fact.

BIBLIOGRAPHY

- Andrew, J.W. Ph.D. Thesis, University of Alberta.
- Andrew, J.W. and Sheinin, S.S. (1974A), Proc. 8th Internat. Conf. on Electron Microscopy, Canberra, 1, p.338.
- Andrew, J.W. and Sheinin, S.S. (1975), Phys. Stat. Sol.(b) 67, 355
- Bethe, H.A. (1928), Ann. d. Physik 87, 55.
- Blackman, M.(1939). Proc. Roy. Soc. A173, 68.
- Boersch, H. (1942). Zeit. fur Physik 118, 706.
- Boersch, H. (1943). Zeit. fur Physik 121, 746.
- Von Borries, B., and Ruska, E. (1940). Naturewiss. 28, 366.
- Cann, C.D.(1973). Ph.D. Thesis, University of Alberta.
- Cann, C.D. and Sheinin S.S.(1974A), Phys. Stat. Sol.(a) 26 193.
- Cann, C.D. and Sheinin, S.S.(1974B), Phys. Stat. Sol.(a) 26, 681.
- Cann, C.D. and Sheinin, S.S.(1972), Phys.Stat. Sol(a) 14, 663.
- Dederichs, P.H. (1972), Adv. Solid State Phys. 27, 135.
- Dupouy, G., Perrier, F., Uyeda, R., Ayroles, R., and Mazel, A. (1965). J.Microscopie 4, 429.
- Davisson, C.J. and Germer, L.H. (1927), Nature 119, 558.
- Doyle, P.A. and Turner, P.S.(1968), Acta. Cryst A24, 390.

- Fujiwara, K. (1962), J.Phys. Soc. Japan 17, 118.
- Fujimoto, F. (1959), J. Phys. Soc. Japan 14, 1558.
- Goringe, M.J., Howie, A., and Whelan, M.J.(1966), Phil. Mag. 14, 217
- Gjonnes, J. and Hoier, R.(1971), Acta. Crystal. A27, 313
- Humphreys, C.j., and Hirsch, P.B.(1968), Phil. Mag. 18, 115
- Humphreys, C.J., and Fisher, R.M.,(1971), Acta. Crystal. A27, 42.
- Heidenreich, R.D.(1942), Phys. Rev. 62, 291
- Heidenreich, R.D., and Sturkey, L. (1945), J.App. Phys. 16, 97
- Heidenreich, R.D.(1949), J. Appl. Phys. 20, 993
- Heidenreich, R.D.(1962), J. Appl. Phys. 33, 2321
- Hirsch, P.B., Howie, A., Nicholson, R.B., Pashley,D.W. and Whelan, M.J. (1965). Electron Microscopy of Thin Crystals(London:Butterworths)
- Howie, A. and Whelan, M.J. (1960), Proc. Eur. Regional Conf. on Electron Microscopy, Delft, p.181
- Howie, A. and Whelan, M.J. (1961), Proc. Roy. Soc. A263, 217
- Howie, A. (1962) J. Phys. Soc. Japan, Suppl. BII, 17, 122
- Howie, A. (1966), Phil. Mag. 14, 223
- Hall, C.R. and Hirsch, P.B. (1965), Proc. Roy. Soc. A286, 158

- Hashimoto, H., Howie, A. and Whelan, M.J. (1962), Proc. Roy. Soc. A269, 80
- Hashimoto, H. (1964), J. Appl. Phys. 35, 277
- Head, A.K., Humble, P., Clarebrough, Morton, A.J. and Forwood, C.T. (1973), Computed Electron Micrograph and Defect Identification (Amsterdam: North Holland Publ. Co.)
- Hillier, J. and Baker, R.F. (1942), Phys. Rev. 61, 722
- Ibers, J.A. (1962), J. Phys. Soc. Japan 17, Suppl. B.II, 4
- Ibers, J.A. and Vainshtein, B.K. (1962), International Crystallographic Tables, Vol. III (Birmingham: Kynoch Press).
- IMSL (1979), International mathematical and statistical Libraries, Inc. (Houston, Texas).
- Kambe, K. and Molière, K. (1970), In Advances in Structure Research by Diffraction Methods, Edited by R. Brill and R. Mason (London: Pergamon Press), p. 53
- Knoll, M. and Ruska, E. (1932), Ann. d. Physik 12, 607
- Kinder, E.(1943). Naturwiss. 31, 149
- Kato, N. (1952), J. Phys. Soc. Japan 7, 397
- Lally, J.S, Humphreys, C.J., Metherell, A.J.F. and Fisher, R.M.(1972), Phil. Mag. 25, 321
- MacGillavry, C.H. (1940), Physica 7, 329
- Pinsker, Z.G. (1953), Electron Diffraction , Translated by

J.A. Spink and E. Feigh (London:Butterworths
Scientific Publications)

Radi, G. (1970), Acta. Cryst. A26, 41

Sheinin, S.S. and Andrew, J.w. (1974), Phys. Stat.
Sol.(b) 61, K13

Sheinin, S.S. and Cann, C.D. (1973), Phys. Stat. Sol.(b)
57, 315

Serneels, R. and Gevers, R. (1972), Phys. Stat. Sol.(b)
50, 99

Serneels, R. and Gevers, R. (1973A), Phys. stat. Sol.(b)
55, 335

Serneels, R. and Gevers, R. (1973B), Phys. Stat. Sol.(b)
56, 681

Sprague, J.A. and Wilkins, M. (1970), Proc. 7th Internat.
Conf. Electron Microscopy 1, 95

Thomson, G.P. and Reid, A. (1927), Nature 119, 890

Thomas, L.E. (1972), Phil. Mag. 26, 1447

Yoshioka, H. (1957), J. Phys. Soc. Japan 12, 618

Whelan, M.J. and Hirsch, P.B. (1957), Phil. Mag. 2, 1121,
1303

Whelan, M.J. (1965A), J. Appl. Phys. 36, 2099

Whelan, M.J. (1965B), J. Appl. Phys. 36, 2103

B30348